Modified error diffusion in colour copying and printing

Tenthof, M.G.J.

Award date:
1996

EINDHOVEN UNIVERSITY OF TECHNOLOGY
FACULTY OF ELECTRICAL ENGINEERING
MEASUREMENT AND CONTROL DIVISION

Modified error diffusion in colour copying and printing

by M.G.J. Tenthof

Report of graduation work (censored version),
performed at Océ van der Grinten N.V., from August 1995 until March 1996.

Océ supervisor: Ir. R. van Strijp
TUE supervisors: Prof. dr. ir. P.P.J. van den Bosch and ir. N.G.M. Kouwenberg

Samenvatting

Ten einde full colour documenten te reproduceren op bijvoorbeeld digitale kopieerapparaten of printers, moet het origineel vele transformaties ondergaan voordat een reproduktie van hoge kwaliteit kan worden verkregen. Een belangrijke transformatie is de conversie van de originele continue kleur informatie naar binaire informatie, noodzakelijk voor reproduktie op de meeste kopieerapparaten en printers. In dit verslag worden verschillende van deze zo genoemde 'halftoon technieken' onderzocht.

Allereerst wordt een overzicht van de meest voorkomende halftoon technieken gegeven. Hieruit volgt dat optimale kwaliteit van het gereproduceerde document wordt verkregen indien de halftoon techniek printbare, i.e. goed reproduceerbare, onregelmatige patronen genereert. Aangezien error diffusion zeer fijne, hoog frequente patronen produceert wordt deze techniek als uitgangspunt voor verder onderzoek genomen. Aangetoond wordt dat toepassing van puur error diffusion op het (kleuren) print engine, niet aan de voorspelde verwachtingen voldoet. Randen en detail informatie worden zeer goed weergegeven terwijl egale vlakken in een zeer ruisachtige indruk resulteren. Ten einde de kwaliteit van de kopie te verbeteren zijn verschillende modificaties van het error diffusie algoritme onderzocht.

Indien de threshold van error diffusie wordt gemoduleerd met de output van al reeds gehalftoonde pixels kunnen de patronen in het output beeld worden geclusterd, hetgeen in beter reproduceerbare output beelden resulteert. Alhoewel scherpe resultaten worden verkregen is betrouwbare kleurmenging niet mogelijk en introduceert toepassing van het algoritme nieuwe zichtbare artefacten welke door de instabiliteit van het algoritme niet goed zijn te controleren. Door de threshold te moduleren met een dither matrix kunnen zowel scherpe en goed reproduceerbare kopieën als een betrouwbare kleurmenging worden verkregen. Door de mate van threshold modulatie te regelen met een rand detector kunnen rand en detail informatie scherp en egale beeldinformatie stabiel worden weergegeven.

Summary

In order to reproduce high quality full colour documents on for instance digital copiers or printers, the original document is subject to many transformations and conversions. An important transformation is the encoding of the original continuous tone information to binary information, needed for reproduction on most marking devices. In this report several of these so called 'halftone techniques' are examined.

First of all an overview of the most commonly used halftone techniques is given. It is concluded that in order to obtain optimum image quality a halftone algorithm should produce printable, i.e. good reproducible, irregular structures. Since error diffusion produces very fine, high frequency patterns it is taken as a starting-point for further investigations. It is shown that application of pure error diffusion on the (colour) print engine does not result in the optimum image quality this technique presumes. Although edges and detail information are rendered very well, application of pure error diffusion results in a visually disturbing noisy impression when smooth or slowly varying image information needs to be rendered. In order to improve image quality several modifications to the error diffusion algorithm are examined.

By modulating the error diffusion threshold with an output dependent feedback term the output patterns are slightly coarsened in order to obtain better reproducible output images. Although the edge rendering properties of error diffusion were maintained, reliable and artifact free colour mixing showed to be impossible and does application of this technique introduce new visually disturbing artifacts which can not reliably be controlled because of the instability of the algorithm. When the error diffusion threshold is modulated with a dither matrix however, sharp and good reproducible output images as well as reliable colour mixing is obtained. By adjusting the amount of threshold modulation with an edge operator it is possible to render edge and detail information sharp and smooth or slowly varying information stable.

Contents

Chapter 1

Introduction

When in the second millennium before the start of our era the alphabet evolved from the hieroglyphs, which was already used by the ancient Egypts, it became possible to transport and hand down stories, messages and ideas etc.. In the fifteenth century the first experiments with printing were performed and circulation of the written word became possible. Till then copying and reading of books was only predestined to the ecclesiastical and juridical class. As the art of printing and reproduction technologies improved over the centuries more and more books and newspapers as well as all kinds of periodics came in circulation. The printed word became one of the most important information sources as well as an important way to relax and enrich oneself.

Nowadays it is almost impossible to imagine a world in which books or newspapers do not exist. Each day we are deluged with brochures and many other black and white, but mostly full colour printed information. Besides the original black and white reproduction technologies, demands for full colour reproduction techniques are increasing. Traditionally these colour documents are reproduced by means of offset printing. The tremendous development over the last decades in computer industry however, has resulted in an increasing number of tools that offer the possibility to work with colours. Since more and more people are making use of these tools apparatus to produce colour documents, like colour copiers and printers, are also needed. In order to transform the continuous tone information in a reliable and cost effective way to for example paper, different techniques have been developed. These techniques transform the continuous tone information, obtained from the original, to binary information, thereby maintaining maximum image quality of the reproduced documents.

This report deals with the 'encoding' of full colour continuous tone documents for reproduction on bi-level printing systems, like copiers and printers. The most common so called 'halftone techniques' together with their properties are discussed. Circumstantial attention is paid to the error diffusion algorithm as well as to several modifications of this algorithm. The different algorithms are implemented in software and tested on a digital full colour copier and printer.

In chapter 2 the functional elements in a digital full colour copier are described, thereby explaining the realisation of reproduced images on a full colour copier. An overview of the different halftone techniques is given in chapter 3. All basic halftone techniques are discussed while special attention is payed to a specific halftone technique called error diffusion. Since application of this halftone technique should result in visually very pleasing patterns it is taken

as a starting-point for further examination. The textures resulting from the error diffusion algorithm are although pleasing for the human eye, very hard to reproduce on many print engines. In order to maintain the advantages of the error diffusion algorithm, while at the same time eliminating the visually disturbing artifacts resulting from limitations of the printing process, several modifications to the error diffusion algorithm are examined. Chapter 4 deals with an output dependent feedback term added to the error diffusion algorithm. The influence on image quality of the weight of this output feedback term, called hysteresis, is described. In order to maintain the stability offered by ordered dither techniques, error diffusion with periodic threshold modulation is discussed in chapter 5. In chapter 6 a classification of the different halftone techniques is given and conclusions with respect to the applicability of the modified error diffusion algorithms are drawn.

Chapter 2

Functional description of a digital full colour copier

This chapter remains Océ property and is therefore only included in the Océ report.

Chapter 3

Survey of the key halftone techniques

When full colour images are reproduced the devices used for rendering these images, like copiers, laser printers and facsimile machines, are in most cases only capable of printing bi-level. So the image information, which is gathered by the scanner and normally represented by values between 0 (solid-tone) and 255 (white), needs to be reproduced by the presence or absence of ink on a page. The encoding technique which converts the continuous-tone images in binary images is commonly called halftoning. Spatial integration and higher-level processing performed by the human eye and brain, and local area coverage of coloured and white pixels provide the appearance of a continuous-tone image at normal reading distance (about 35,6 centimetre). Different techniques for encoding these continuous-tone images will be discussed in the next paragraphs ([Stof81], [Uli87], [Dou94], [Jon94]).

3.1 Traditional Screening

Already in the 19th century the first experiments (Talbot 1852) with halftoning were performed. In order to reproduce the image of an object a so called photoengraving process was used. See figure 3.1.

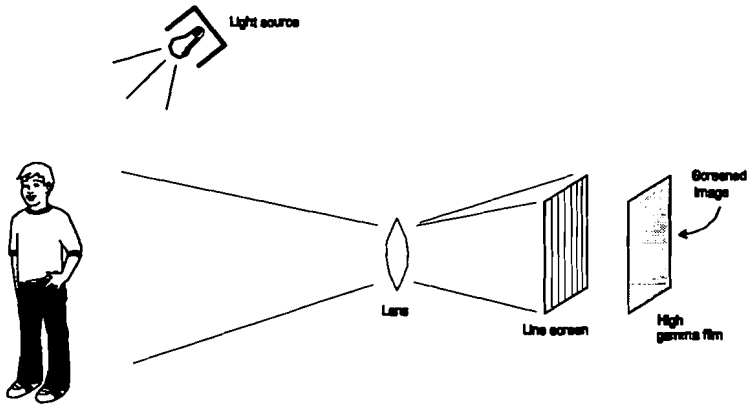

Figure 3.1: Fundamentals of traditional screening.

Between the lens and the photosensitive plate a transparent screen with ruled lines was placed. Upon exposure the original image has superimposed on it the density function of the transparent screen, resulting in an intensity modulation that is sensed by the high gamma film. After chemical development of the film it results in a binarized image which has, because of the spatial integration performed by the human eye, the continuous-tone appearance of the original. Figure 3.2 shows a simplified schematic view of the above described procedure.

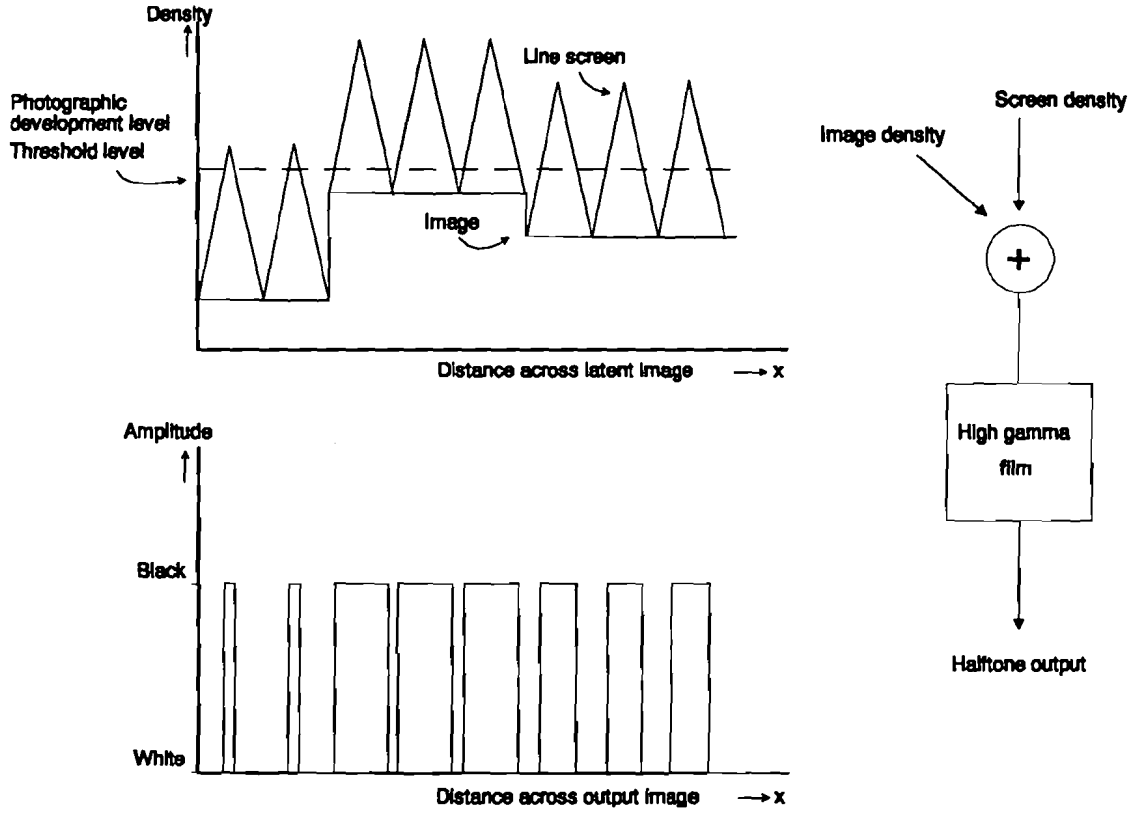

Figure 3.2: Schematic view of traditional screening.

A lot of effort was put in simplification of the screening process and improvement of the resulting image quality. This resulted in rotated screen rulings and combinations of different screens for the reproduction of colour prints and finally led to the invention of the contact screen. With the invention of the contact screen careful spacings between the screen and the high gamma film were no longer required and diffraction was no longer a degrading factor.

3.2 Ordered dither

An ordered dither technique is in fact the digital analog of the photomechanical process described in paragraph 3.1. In figure 3.3 a schematic view of the ordered dither process is depicted. In order to obtain the binary output of the halftoned image sampled continuous-tone picture elements are compared with a threshold, which is selected in sequential order from a two-dimensional matrix, defined to be the halftone cell threshold set, also called the dither matrix.

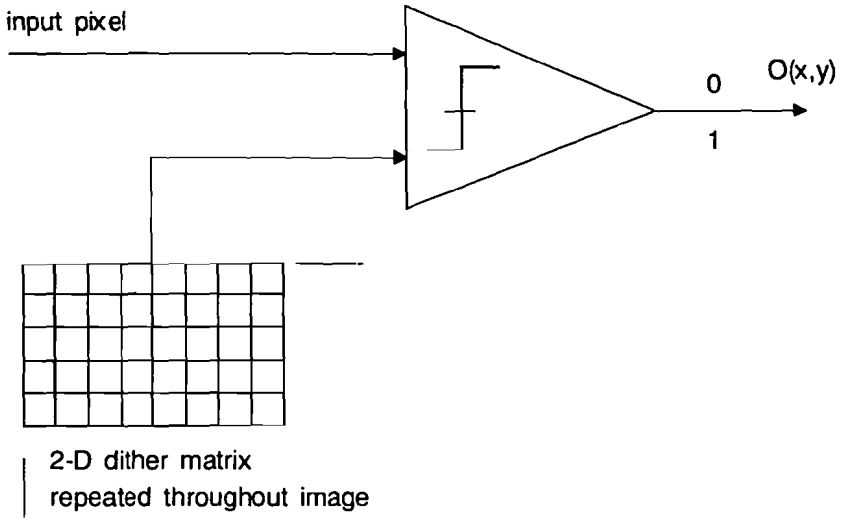

Figure 3.3: Schematic view of the ordered dither process.

Hence, techniques that repeat the dither matrix periodically throughout the image plane, thereby using the thresholds in the dither matrix in a sample-by-sample comparison algorithm to obtain the halftoned output image are called ordered dither techniques. The decision of printing or not printing ink depends on the outcome of the comparison. See figure 3.4.

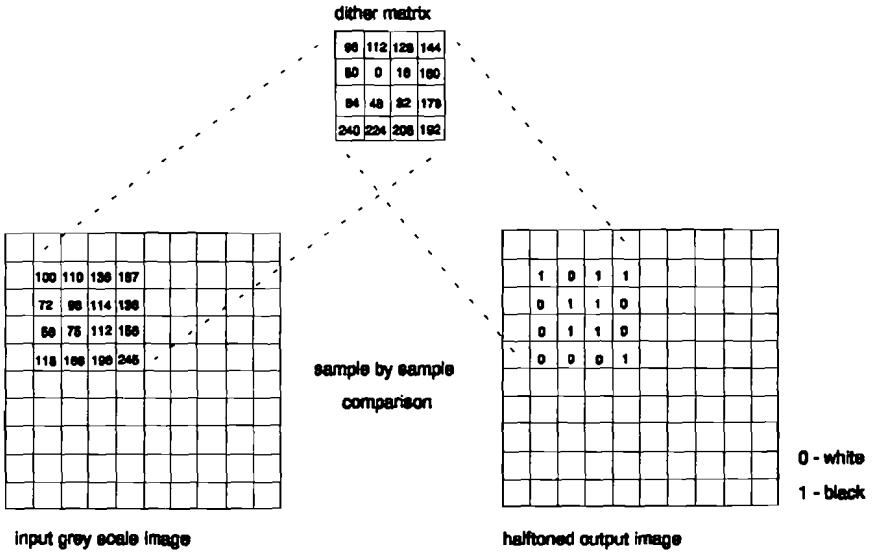

Figure 3.4: Sample-by-sample comparison.

The halftone operation can be written as

$$b(x,y) = \begin{cases} 0, & f(x,y) < T_{mn}(k,l) \\ 1, & f(x,y) \geq T_{mn}(k,l) \end{cases}, \qquad (3.1)$$

where $b(x,y)$ is the halftoned output,
$f(x,y)$ is the sampled continuous-tone image,
$T_{mn}(k,l)$ is the dither matrix with dimensions m and n and
$k = x \bmod m$ and $l = y \bmod n$.

It is noted that the number and arrangement of the thresholds in the dither matrix determine the grey (or colour)-scale range, the screen frequency and screen angle of the resulting halftoned image.

When a constant tone value is halftoned with a dither matrix which has only one seed it results in a repeating pattern, determined by the arrangements of the thresholds in the matrix, with a period equal to the size of the dither matrix. On the other hand, ordered dither techniques will preserve sharp edges and discontinuities at the correct pixel locations. Especially the high-contrast edges will be rendered very well, because well defined transitions are easily 'detected' by the local thresholds.

Ordered dither techniques can be divided into two groups: clustered dot and dispersed dot ordered dither techniques. Clustered dot ordered dither techniques try to group the individual dots into larger spatial units and are applied when printing devices are not capable of reliably printing individual halftone dots. Dispersed dot ordered dither techniques turn individual halftone dots on or off without trying to group them into clustered areas. These dither techniques are used in binary displays and printing devices that can reliably print individual halftone dots.

3.2.1 Clustered dot ordered dither techniques

Clustered dot ordered dither techniques, also called Amplitude Modulation screening or Dot Size Modulation, are nowadays the most widely employed halftoning techniques in the digital printing industry. In essence it is the sampled equivalent of the traditional screening process. When a clustered dot ordered dither technique is applied the tone value of a sampled picture element is represented by modulation of the size of the halftone dots. In figure 3.5 the principle of the clustered dot ordered dither technique is shown.

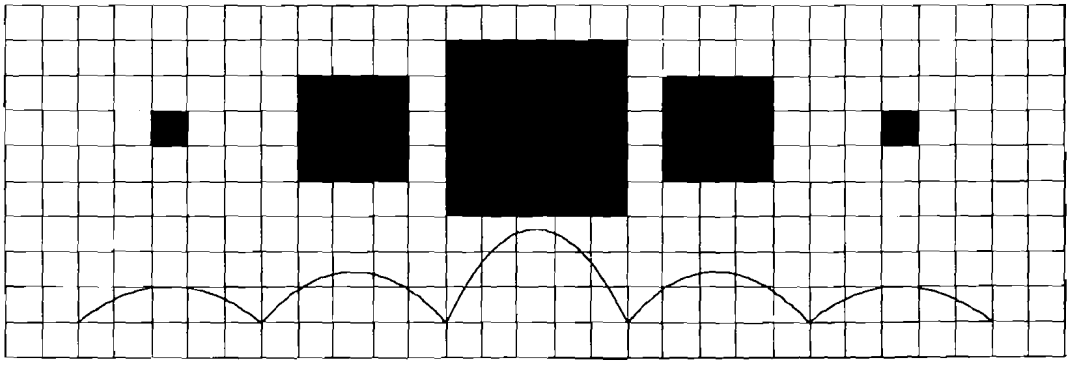

Figure 3.5: Principle of the clustered dot ordered dither technique.

Figure 3.5 shows that when the tone value of a sampled picture element, represented by the amplitude of the waveform, becomes higher the size of the halftone dot becomes bigger or vice

versa. It is noted that for a clustered dot ordered dither technique it is characteristic that the distance between the centres of the halftone dots is constant.

With clustered dot ordered dither techniques tone reproduction with devices that have a nonlinear reflectance response, i.e. the reflectance is not equal to the ratio of the number of white pixels to the total number of pixels in the dither matrix, can be optimized. By clustering the individual halftone dots maximum overlap is forced and dot shape and size influences are minimized. See figure 3.6.

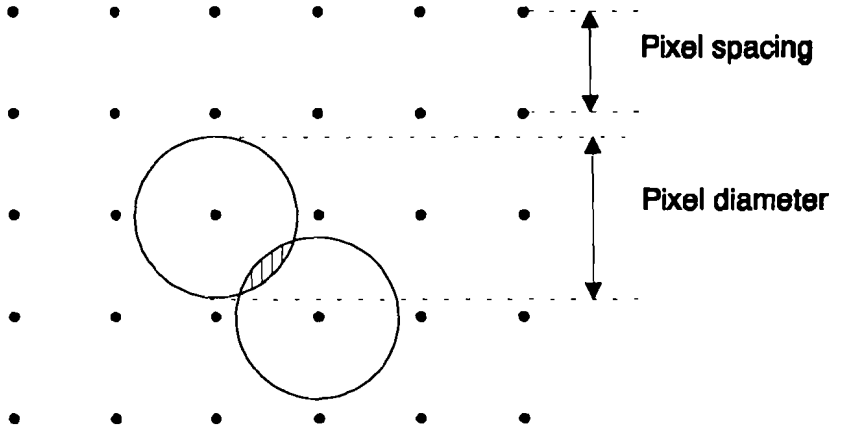

Figure 3.6: Illustration of minimizing the influences of dot size and shape on the reflectance response.

As was mentioned before, the number and arrangement of the thresholds in the dither cell, the cell size and shape and the offset of successive rows of dither cells, determine the tone-scale range, screen frequency and screen angle of the resulting halftoned image.

The dimension of the dither matrix determines the number of tone values that can be represented. An 8 x 8 matrix for instance, can reproduce 65 tone values (64 tone values and white). So, in order to reproduce a halftoned image free of false contours and with the same apparent tone rendition as the original image, the dimensions of the dither matrix should be large enough to make it possible to render tone value steps that can not be distinguished by the human eye. Furthermore, the threshold values themselves and the fill order of the dither matrix are important. Since the human eye is more sensitive to tone value steps in highlight regions than in midtone or shadow regions, the values of the thresholds in the dither matrix should be chosen such that a maximum of tone values can be rendered in the highlight regions. A commonly used technique to determine the threshold values is by measuring the reflectances R_i ($0 \leq R_i \leq 1$ with $i \in [0, p]$ and p the number of thresholds in the dither matrix) for each possible pattern in the dither matrix. The desired threshold can now be determined according to

$$t_n = \frac{M(R_{p-n+1} + R_{p-n})}{2}, \qquad (3.2)$$

where t_n represents the threshold value,
n represents the fill order ($0 \leq n \leq p$) and
M is the largest digital value of image reflectance (i.e. 255 for 8 bits/ pixel).

By carefully choosing the growth pattern in the dither cell the screen frequency and screen angle can be determined. By using dither cells which have typically two or four seeds that grow alternatingly in a spiral form, the apparent screen frequency can be increased. Because the dot density is increased this way, the halftoned images contain less low frequency components which is pleasing for the human eye. It is noted that because of the alternating dot growth the tone value step size becomes larger than in case of single dot growth, which can result in slight texture in the highlight regions. In equation 3.3 an example of a quad-dot dither matrix is shown.

$$T_{12,8} = \begin{bmatrix} 158 & 215 & 144 & 44 & 30 & 72 & 165 & 222 & 151 & 51 & 37 & 79 \\ 126 & 97 & 111 & 175 & 190 & 133 & 119 & 90 & 104 & 183 & 197 & 140 \\ 12 & 26 & 69 & 232 & 247 & 204 & 5 & 19 & 62 & 239 & 254 & 211 \\ 55 & 40 & 83 & 161 & 218 & 147 & 48 & 33 & 76 & 168 & 225 & 154 \\ 179 & 193 & 136 & 122 & 94 & 108 & 172 & 186 & 129 & 115 & 87 & 101 \\ 236 & 250 & 207 & 8 & 23 & 65 & 229 & 243 & 200 & 2 & 16 & 58 \end{bmatrix}. \quad (3.3)$$

In order to minimize disturbing visual patterns screens are in practice given an offset angle. By giving the dither cells an offset in horizontal direction when tiling the continuous-tone image the specific screen angle can be realized, see figure 3.7.

Especially when colour prints need to be reproduced an overlay of three colour separation images, each halftoned, is needed. Since the spectra of these different colours are partially overlapping it will result in objectional low-frequency interference patterns, called moiré. To minimize the visibility of these patterns the different colour screens are typically oriented about 30 degrees apart.

When the clustered ordered dither technique is applied it is desirable to be able to print as many tone values as possible (about 100 levels for high quality halftoning). In order to realize this large number of tone values 'large' dither cells are needed. On the other hand it is also desirable to maximize the screen frequency, which can be achieved by applying more seeds in one dither cell. Hence, by increasing the number of pixels in the dither matrix it is possible to represent more tone values, thereby decreasing the likelihood of false contours. A consequence of an increasing cell size for single clustered dots is that the screen will contain more low frequency components and therefore becomes coarser and more visible and is also less capable of representing fine detail. When the number of pixels for one single clustered dot decreases the apparent screen frequency becomes higher and the screen will be less visible and finer detail can be represented. So a trade-off is necessary between the screen frequency and the number of tone values that can be represented.

In summary it can be stated that clustered dot ordered dither is widely used because of its simplicity and speed. Screen visibility when low resolutions are used, problems with rendering smooth edges and moiré are the disadvantages of this ordered dither technique.

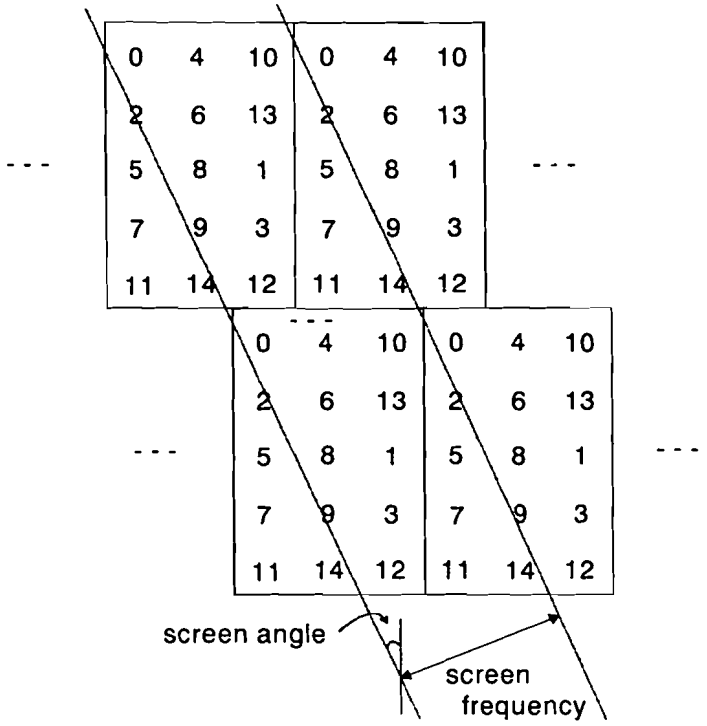

Figure 3.7: Construction of angled halftone screens with rectangular dither cells.

3.2.2 Dispersed dot ordered dither techniques

When dispersed dot ordered dither, also called Frequency Modulation screening, Random screening, Random dithering, Stochastic screening or Diamond screening, is applied the tone value of a sampled picture element is represented by modulation of the number halftone dots per centimetre. See figure 3.8.

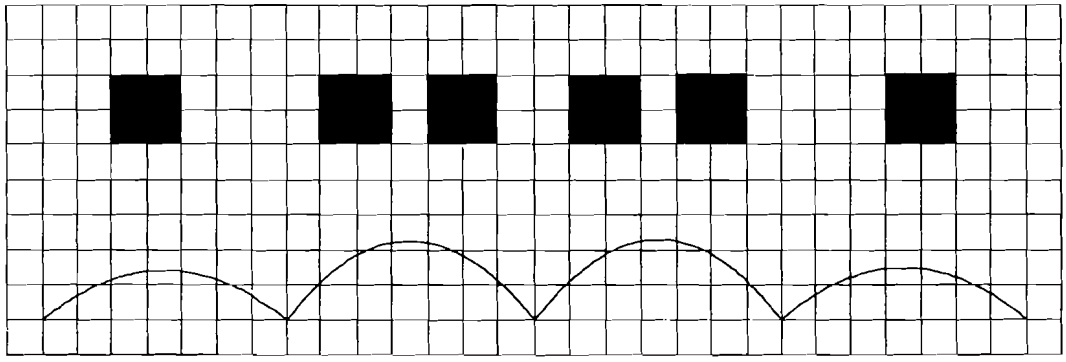

Figure 3.8: Principle of Frequency Modulation screening.

It is mentioned that dispersed dot ordered dither is not possible with the conventional photographic processes described in paragraph 3.1, but can only be produced electronically.

With dispersed dot ordered dither the halftone dots are, in contradistinction to the halftone dots used with clustered dot ordered dither, of constant size. In fact the only difference to clustered dot ordered dither is that the placement of the halftone dots is nearly random, i.e. as isolated small dots instead of as a coherent area. With dispersed dot ordered dither the screen frequency, the number of halftone dots per centimetre, actually changes throughout the image. Consider for example the dot arrangements shown in figure 3.9[a] and 3.9[b], both representing a tone value of 25%.

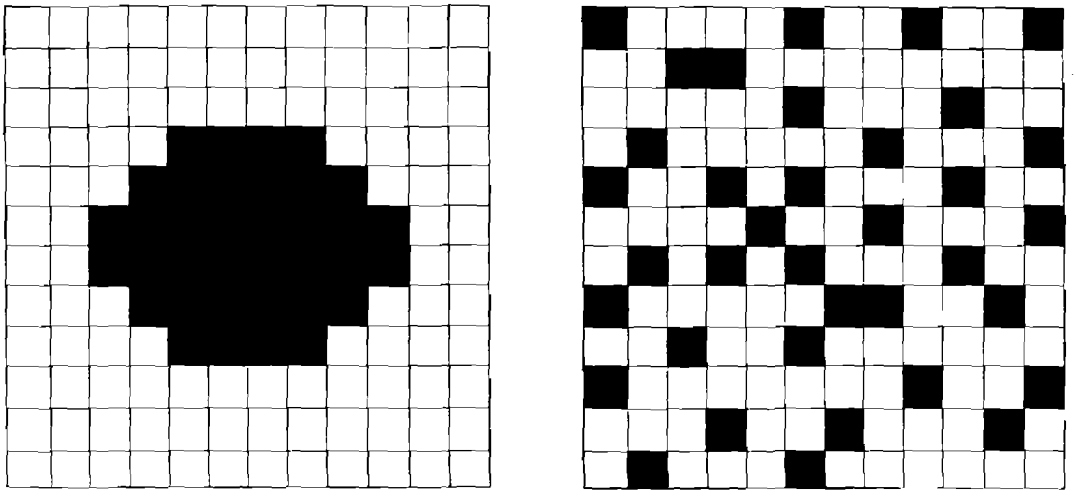

Figure 3.9: Tone value of 25% for dot arrangement used in clustered dot (a) and dispersed dot ordered dither (b).

The easiest way to implement a clustered or dispersed dot ordered dither technique is by defining for each tone value one (or more) dot arrangement(s) in the form of a bitmap and store them into the data memory. However, in practice this would result in an overloaded data memory and therefore clustered as well as dispersed dot ordered dither techniques are in most cases implemented by specific arrangements of the thresholds in the halftone cell.

When devices that can reliably reproduce individual pixels or devices with an approximately linear system response are used, dispersed dot order dither techniques can be very useful. These techniques have the attractive properties, like speed and simplicity, of ordered dither techniques but produce patterns that do not suffer the strong horizontal and vertical structures of clustered dot ordered dither. Some important dispersed dot ordered dither techniques will be presented below.

Bayer dither

The thresholds in the dither matrix are arranged to minimize low-frequency texture in the halftoned image. The criteria that result in dither cells with minimum low-frequency content are derived by Bayer [Bay73]. According to Bayer it is supposed that a uniform grey area is represented by repeating both horizontally and vertically a 2^m by 2^m subarray of black and white elements, i.e.

$$b(x+2^m,y) = b(x,y+2^m) = b(x,y), \tag{3.4}$$

where $b(x,y)$ represents the halftoned output (0 or 1) at column x and row y of the picture lattice. When all combinations of integers x and y ($0 \le x < 2^m$ and $0 \le y < 2^m$) define the basic subarray, the function $b(x,y)$ can be represented by the following Fourier series

$$b(x,y) = \sum_{u=-I+1}^{I} \sum_{v=-I+1}^{I} F(u,v)\, e^{-2\pi i\left(\frac{ux+vy}{2^m}\right)}, \tag{3.5}$$

where $I = 2^{m-1}$ and x and y are integers. The Fourier coefficients $F(u,v)$ can now be written as

$$F(u,v) = \frac{1}{2^{2m}} \sum_{x=0}^{2^m-1} \sum_{y=0}^{2^m-1} f(x,y)\, e^{2\pi i\left(\frac{ux+vy}{2^m}\right)}, \tag{3.6}$$

with u and v integers. The real part of each term in equation 3.5 is a plane wave with amplitude

$$A(u,v) = \sqrt{F(u,v)\,\overline{F(-u,-v)}}, \tag{3.7}$$

and a wavelength, measured at right angles to the wavefront, that can be written as

$$\lambda(u,v) = \frac{2^m}{\sqrt{u^2+v^2}}. \tag{3.8}$$

It is clear that only the components with nonzero amplitude, $A(u,v)$, and finite wavelength, $\lambda(u,v)$, contribute to the appearance of texture. It is therefore that Bayer defines the index for texture in a uniform area, Λ, as the longest finite wavelength of the nonzero-amplitude plane wave components of the dot pattern. Hence, the measure for texture is defined as

$$\Lambda = Max\{\lambda(u,v) \mid \lambda(u,v) \neq 0,\ \lambda(u,v) < \infty\}. \tag{3.9}$$

Since the impression of texture is mainly based on the patterns having the largest value of Λ, the preferred dither cell is defined such that Λ of the resulting halftoned image is as small as possible for all tone values that can be represented. In order to satisfy this optimization criterion Bayer derives a set of conditions that a sequence of lattice positions must met.

It is supposed that each new pattern is obtained from the last by adding one black dot to an empty position in a 2^m x 2^m subsection of the lattice. When k represents the number of black dots in a printed cell, which is halftoned by a threshold array T with dimensions 2^m x 2^m and for each k $(0 \le k \le 2^{2m})$, 2^n is the largest power of 2 that divides k, the optimality conditions can be written as follows.

1. For even n, b (the halftoned output) must obey

$$b(x+2^{m-\frac{n}{2}},y) = b(x,y+2^{m-\frac{n}{2}}) = b(x,y). \tag{3.10}$$

2. For odd n, b must obey

$$b(x+2^{m-\frac{(n+1)}{2}},y+2^{m-\frac{(n+1)}{2}}) = b(x+2^{m-\frac{(n+1)}{2}},y-2^{m-\frac{(n+1)}{2}}) = b(x,y). \tag{3.11}$$

Bayer proofs that the dither matrix will yield a halftoned image which contains a minimum of texture if and only if the above conditions are satisfied for all k. Under the above conditions the maximum wavelength is given by

$$\Lambda = 2^{m-\frac{n}{2}}, \tag{3.12}$$

for each value of k ($0<k<2^{2m}$).

It is mentioned that the above conditions are equally applicable to the construction of dither cells with dimensions of 2^m x 2^{m-1} lattice positions. Equation 3.13 shows a Bayer dither matrix with which halftoned images that obey the above optimality conditions can be reproduced.

$$T_{Bayer\ dither} = \begin{bmatrix} 0 & 128 & 32 & 160 & 8 & 136 & 40 & 168 \\ 192 & 64 & 224 & 96 & 200 & 72 & 232 & 104 \\ 48 & 176 & 16 & 144 & 56 & 184 & 24 & 152 \\ 240 & 112 & 208 & 80 & 248 & 120 & 216 & 88 \\ 8 & 136 & 40 & 168 & 0 & 128 & 32 & 160 \\ 200 & 72 & 232 & 104 & 192 & 64 & 224 & 96 \\ 56 & 184 & 24 & 152 & 48 & 176 & 16 & 144 \\ 248 & 120 & 216 & 88 & 240 & 112 & 208 & 80 \end{bmatrix}. \tag{3.13}$$

Figure 3.10 shows enlarged versions of a part of a halftoned continuous tone image. The image shown in figure 3.10[a] is halftoned with a clustered dot ordered dither matrix with one seed that grows in a spiral form, and figure 3.10[b] depicts the same image but halftoned with the Bayer dither matrix given in equation 3.13. Figure 3.10 clearly shows the typical patterns that occur when using these different techniques. In order to obtain the same grey value impression for both images a calibration is performed to eliminate the system and printer influences. This is done by measuring the grey value impression (lightness) of a halftoned and printed grey wedge and implementing the inverse transfer function before the halftone and print path.

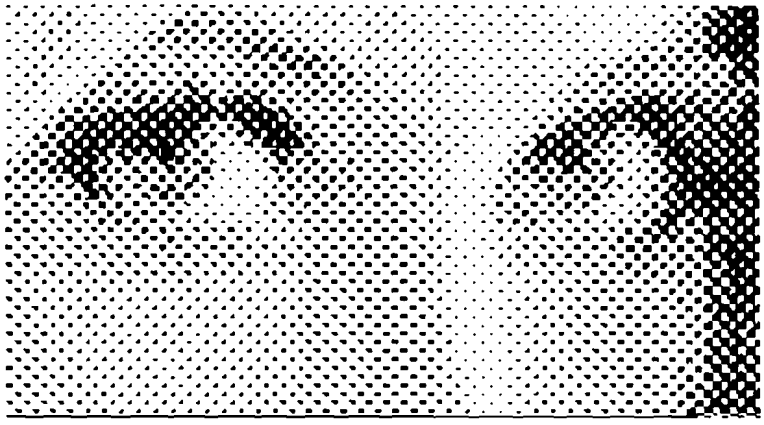

A

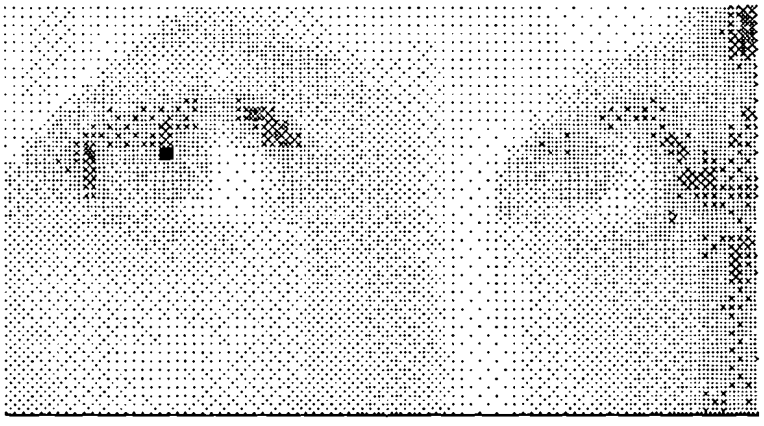

B

Figure 3.10: Example of a continuous-tone image halftoned with the clustered dot ordered (a) and dispersed dot ordered (b) dither techniques

When the Bayer dither matrix is used picture detail is rendered well and a minimum of texture will be produced.

Void and cluster method

Another technique worth mentioning is the void-and-cluster method [Uli93]. This technique also generates dither cells based on the principle of placing the individual dots as far from each other as possible thereby generating patterns to optimize isotropy. The terms 'void' and 'cluster' refer to the arrangement of minority pixels on the background of majority pixels, where for tone values less than 50% ones represent the minority and zeros represent the majority pixels, and vice versa for tone values greater than 50%. So a void is defined as a large space between minority pixels and a cluster is defined as a tight grouping of minority pixels. To produce the desired homogenous patterns minority pixels are always added in the centre of the largest voids and removed from the centre of the largest cluster, maintaining the overall tone impression.

In order to locate voids and clusters in a binary pattern this technique uses a filter which must satisfy the wrap-around property, because of the periodic nature of dither techniques. This means that when the span of this filter extends the bounds of the dither cell, it must wrap around to the other side of the dither cell. The filter considers the neighbourhood around every majority pixel in order to find voids and considers the neighbourhood around every minority pixel to find clusters. It is clear that the choice of the filter is very important for the success of this method. Ulichney uses a two-dimensional Gaussian filter but shows that a variety of filters will work. The two-dimensional Gaussian filter is given by

$$e^{-\frac{x^2}{2\sigma_x^2}-\frac{y^2}{2\sigma_y^2}}, \tag{3.14}$$

where x and y represent the pixel positions and $\sigma_{x,y}$ represent the standard deviation in terms of pixel spacing.

To fill the dither cell the void and cluster technique uses an initial pattern. To generate this initial pattern, which should have a grey value less than 50%, a white noise generator can be used. To produce the initial pattern the minority pixels in the white noise pattern are moved from the tightest cluster to the largest void, thereby reducing the size of the largest void and largest cluster. This is done until removing a one from the largest cluster generates the largest void.

With this initial pattern as starting point the dither cell can be build. For tone values less than 50% the tone value patterns are evaluated from the initial pattern by removing ones from the tightest cluster or by inserting ones in the largest voids. For tone values greater than 50% ones are inserted in the tightest cluster, which is now formed by the zeros. In order to fill the dither matrix the quantity 'rank' is introduced. The rank of a dither matrix element represents the number of ones in the specific tone value pattern minus the one at the location of that element. In order to build the dither matrix it is filled with the rank at the location at which a one is inserted or removed from the tone value pattern, for tone values larger than respectively smaller than the value represented by the initial pattern. It is obvious that the rank needs to be normalized to match the range of input and output values.

The void and cluster method is a technique that has the attractive properties of ordered dither, but lacks the regular structures that result from a clustered dot ordered dither technique. Unlike the Bayer dither technique the void and cluster method is not restricted to dither matrix dimensions that are a power of two, which makes it a general applicable technique. Compared with the error diffusion technique, which will be dealt with in the next paragraph, the void and cluster method produces patterns that are more homogeneous but appear to be less sharp than when error diffusion is used.

Blue Noise Masking

The presence of significant low frequency components is responsible for the visibility of disturbing artifacts in halftoned images. Since the human eye is less sensitive for high frequencies, dither techniques that produce unstructered, high-frequency patterns (at a given resolution) will result in visually pleasing images.

Blue Noise Masking is a dither technique that uses the speed of ordered dither techniques and produces the high quality results of error diffusion techniques. This is realized by constructing a

dither cell such that it has specific first and second order properties ([Par92], [Mit92], [Yao94]). The constrained first order properties result in preservation of the average grey level. Hence, when the mask is thresholded at any level, say at A% of the maximum level, exactly A of every 100 dots will be turned on. The second order properties of the mask are such that the spatial distribution of black and white dots in the halftoned image result in a power spectrum which has blue noise characteristics at each tone value level. The radially averaged power spectrum [Uli87] of a blue noise binary pattern is depicted in figure 3.11.

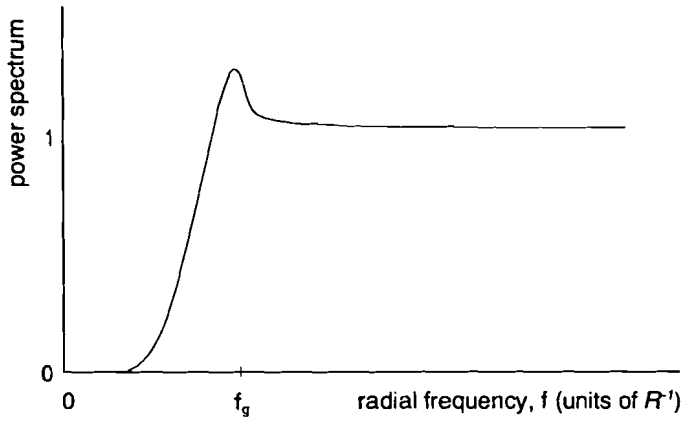

Figure 3.11: Radially averaged power spectrum of a blue noise pattern.

The cut-off frequency, f_g, known as the principal frequency, is given by

$$f_g = \begin{cases} \frac{\sqrt{g}}{R}, & \text{for } g \le 0.5 \\ \frac{\sqrt{1-g}}{R}, & \text{for } g > 0.5 \end{cases} \quad , \tag{3.15}$$

where g represents the tone value level ($0 \le g \le 1$) and
R is the distance between the individual dots (sample period [m]).

Equation 3.15 shows that the cut-off frequency, f_g, of the blue noise power spectrum depends on the tone value. For a tone value of 50% the cut-off frequency is at its highest value because at this value the number of black dots equal the number of white dots resulting in a pattern with the highest frequency components. By minimizing the low frequency components in the power spectrum of the halftoned image the number of spectral orders that are close to the zeroth order, which represents the spectrum of the original image, are minimized. This means that the interference of the zeroth spectral component with these nonzero components is minimized and therefore the visually annoying artifacts in the halftoned image can be minimized.

An important property of the Blue Noise Mask (BNM) is that when it is thresholded at any tone value level g, the resulting binary dot profile, $p(i,j,g)$, has blue noise characteristics. The value of

the dot profile at a particular location *(i,j)*, for tone-value level g is defined by

$$p(i,j,g) = \begin{cases} 1 & g > m_{ij} \\ 0 & g \leq m_{ij} \end{cases}, \tag{3.16}$$

where $m_{i,j}$ represents the mask value of the corresponding pixel in the BNM. The different dot profiles for each level are constructed sequentially, which means that the dot profile for level $g_l + \Delta g$ is constructed from the dot profile for level g_l by changing a predefined number of zeros to ones. Dot profiles for tone value levels lower than the current level are constructed from the current level by changing the same predefined number of ones to zeros. This means that the different dot profiles depend on each other. This dependence can be written as

$$\text{if } g_2 > g_1 \bigcap p(i,j,g_1) = 1 \quad \rightarrow \quad p(i,j,g_2) = 1. \tag{3.17}$$

It is noted that since error diffusion lack this dependence of dot profiles, the overall results obtained with error diffusion are superior to those obtained with Blue Noise Masking. Nevertheless is Blue Noise Masking very interesting because of its speed, when the BNM is constructed it is reduced to a simple dither technique.

In order to build an $M \times N$ B-bit deep BNM, 2^B different dot profiles need to be designed such that the available tone value levels can be represented uniquely. The number of zeros that will change to ones or the number of ones that will change to zeros, when the dot profile for respectively level $g_l + \Delta g$ or level $g_l - \Delta g$ is constructed from the dot profile for level g_l, is equal to $(M \times N).\Delta g$, with $\Delta g = 1/2^B$.

Before the actual BNM can be built a starting dot profile with suitable blue noise characteristics is needed. This starting dot profile is very important for the overall construction of the BNM because all other dot profiles are built from this pattern. Figure 3.12 shows the flow diagram for the construction of the starting dot profile at tone value level $g = g_s$. In practice g_s mostly equals 0.5 when g is normalized to $0 < g < 1$ or g_s equals 128 when g is normalized to $0 \leq g \leq 255$ (assuming 8-bit image planes).

The starting binary pattern can be obtained with for instance a white noise generator. After the starting binary pattern is low-pass filtered, it will in the spatial domain no longer be binary and will thus differ from the original binary pattern. In the spatial domain for each pixel of the filtered pattern the deviation (error) with the average tone value level of the starting binary pattern is determined. For all pixels containing a 1 in the original binary pattern the pixels of the filtered array are found that have the largest positive deviation from the average tone value level and for all pixels containing a 0 in the binary pattern the pixels in the filtered pattern with the largest negative errors are found. The pixels with the largest deviation from the average tone value level represent the centres of the largest clumps, which need to be eliminated in order to obtain visually pleasing patterns. This is done by swapping M ones and M zeros (those with the largest errors) in the original binary pattern. This way a new binary pattern, $p_l(i,j,g_s)$ (with l the l^{th} iteration), is created. The above described process is repeated until a stopping criterion, formed by the Mean Squared Error (MSE) of the filtered pattern with respect to g_s, is satisfied. It is mentioned that the initial value of M needs to be determined experimentally.

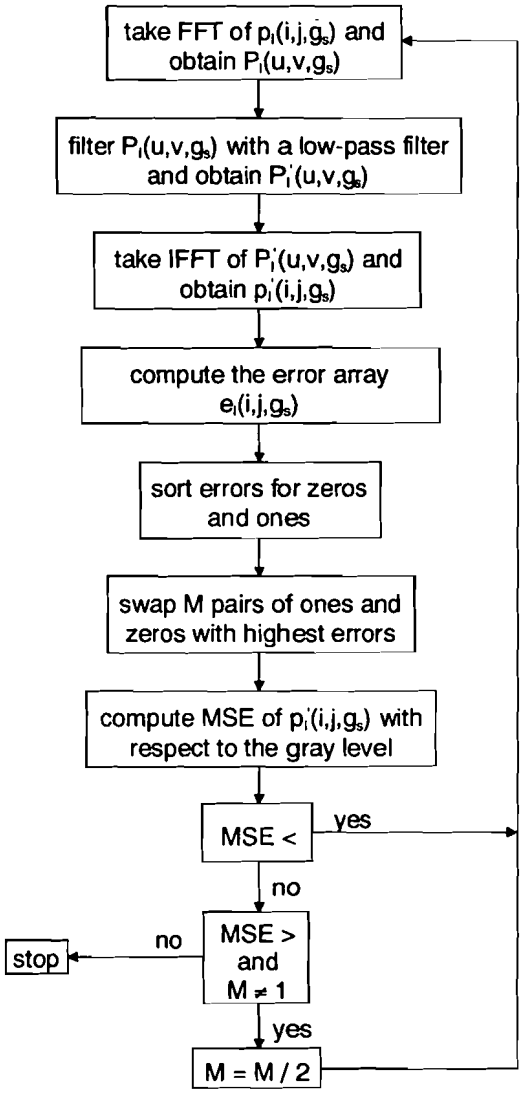

Figure 3.12: Flow diagram for construction of the starting dot profile.

As long as the MSE decreases or the MSE increases but M is still unequal to one the next iteration is processed. First when the MSE increases and M equals one the created dot profile can be used as the blue noise starting pattern $p(i,j,g_s)$.

A smoothly varying low-pass filter that can be used in the above algorithm is the Butterworth filter [Yao94]. The Butterworth filter is given by

$$R(u,v) = \left\{ \frac{1}{1 + \left(\frac{\sqrt{u^2+v^2}}{f_c} \right)^{2N}} \right\}^{\frac{1}{2}}, \qquad (3.18)$$

where u and v are the transform coordinates,
N is the order of the Butterworth filter and
f_c represents the cut-off frequency, which is defined as in equation 3.15
(f_c = *frequency factor x* f_g).

Since with the above algorithm a good blue noise starting pattern can be built, it is now possible to construct the BNM. The flow diagram for the construction of the BNM is depicted in figure 3.13.

It is noted that when the BNM is used to halftone a constant grey level image of level g_s, it produces the initial binary pattern. From the blue noise pattern for level g_s all other dot profiles are constructed by converting the appropriate number of zeros to ones for levels higher than g_s and vice versa for level lower than g_s. After each dot profile is optimized to satisfy the blue noise characteristics the mask is updated. When the mask is updated for all dot profiles, the resulting single-valued function is the BNM.

From the initial binary pattern, $p(i,j,g_s)$, the initial mask is constructed according to

$$m(i,j) = \begin{cases} g_s & \text{for } p(i,j,g_s)=0 \\ g_s-1 & \text{for } p(i,j,g_s)=1 \end{cases}, \tag{3.19}$$

where $p(i,j,g_s)$ is the value of the binary pattern for level g_s at location (i,j),
$m(i,j,g_s)$ is the mask value at location (i,j) and
g_s normalized to $0 < g_s < 255$ (assuming 8-bit image planes).

In order to construct the BNM for $g = g_l > g_s$ the dot profiles for $g_l = g_l + \Delta g$ need to be determined. Each dot profile is constructed from its predecessor, $p_{lk}(i,j,g_l)$ (with k the k^{th} iteration), by converting $(M \times N).\Delta g$ zeros to ones. The obtained pattern $p_{lk}(i,j,g_l + \Delta g)$ is optimized to satisfy the blue noise characteristics in exactly the same way as described for the starting pattern. See also figure 3.13. If the optimized dot profile, $p_{lk}(i,j,g_l + \Delta g)$, is obtained the mask can be updated.

This is done according to

$$m(i,j) = m(i,j) + \overline{p(i,j,g_l+\Delta g)}, \tag{3.20}$$

where the bar indicates the NOT operation. This process is repeated until a grey value equal to or lager than 255 is obtained. The mask is now updated for a grey levels larger than g_s.

For grey values smaller than g_s the same procedure as described above can be applied, with the status of the zeros and ones converted. The initial dot profiles for grey values $g_l - \Delta g$ are now obtained by converting $(M \times N).\Delta g$ ones to zeros. When the dot profile $p_{lk}(i,j,g_l - \Delta g)$ satisfies the blue noise characteristics the mask is updated according to

$$m(i,j) = m(i,j) - p(i,j,g_l+\Delta g). \tag{3.21}$$

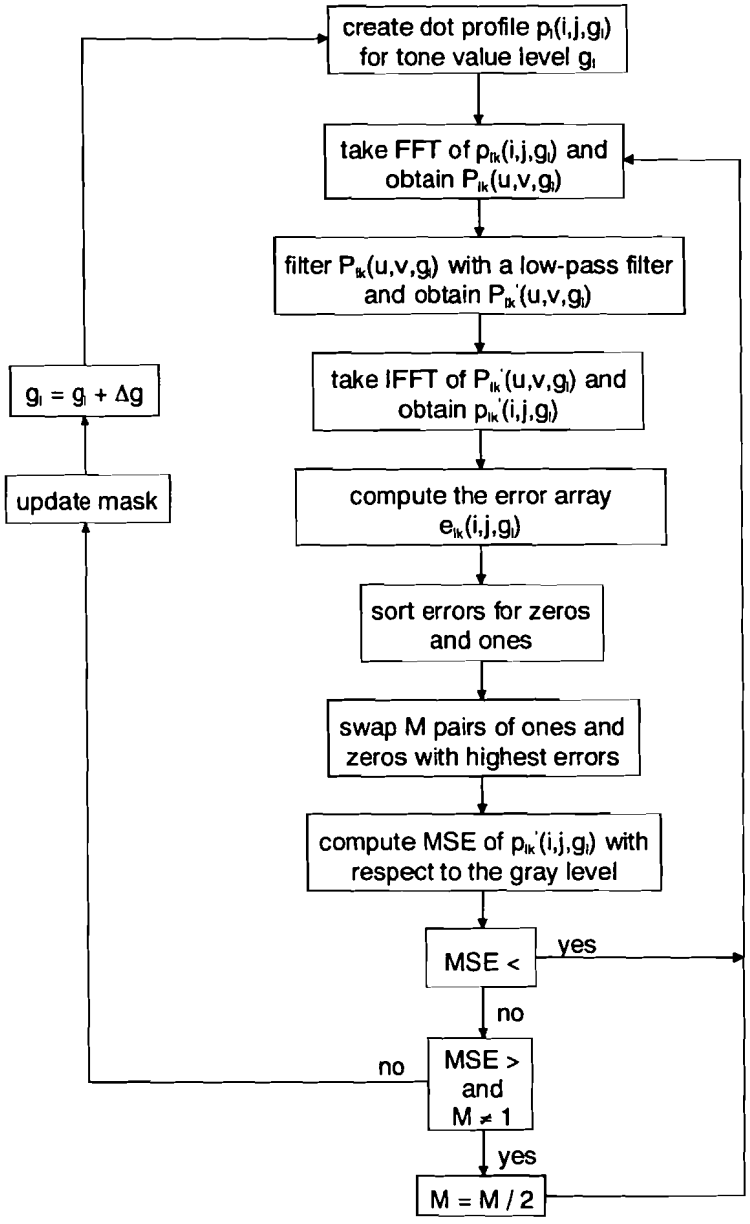

Figure 3.13: Flow diagram for construction of the BNM.

The construction of the mask is complete when it is updated for all possible grey levels. An image can now be halftoned by repeating the mask in both horizontal and vertical direction and applying equation 3.16 to each pixel position of the image plane.

When a dot profile is constructed from its predecessor, at random positions a predefined number of zeros is changed to ones or vice versa. It is stressed that the algorithm described above will switch locations during the iteration process in order to avoid clumps and therefore obtains patterns that satisfy the blue noise characteristics. A significant constraint on the algorithm is

however that when switching locations the ones (upward construction) shared by two neighbouring levels can not be changed to zeros. So, when the dot profile for g_i contains a one at location *(i,j)* all dot profiles for higher grey levels contain a one at that location. This constraint on the BNM makes error diffusion superior to Blue Noise Masking. See also equation 3.17.

The dispersed dot ordered dither techniques as described above are very popular in offset printing were resolutions larger then 1200 dots per inch (dpi) are applied. At these high resolutions dispersed dot ordered dither shows, with respect to clustered dot order dither, the following advantages ([Sch84], [Wid92]):

- smoother transitions in tone rendering,
- better detail rendering and
- no moiré patterns and no need for screen angles.

It is mentioned that when using dispersed dot ordered dither techniques there are some important requirements to the apparatus used:

- the ability to reproduce very small halftone dots (resolutions below 600 dpi have a tendency to graininess) and
- for most applications more processing power is needed in order to calculate the positions of the individual halftone dots.

3.3 Error diffusion

Opposed to the dither techniques described in the preceding paragraphs error diffusion is a technique in which the already processed neighbourhood pixels influence the halftoned output of the pixel under process ([Uli87], [Uli88], [Kno93'], [Dou94]).

3.3.1 Basic error diffusion algorithm

The halftoned output of a continuous-tone image is in error diffusion obtained by thresholding each pixel at a (fixed) threshold level T. When thresholding an image pixel an error, represented by the difference between the halftoned output (zero or one) and the grey level of the input pixel (normalized to $0 \leq g \leq 1$), occurs. The main characteristic of error diffusion is that this error is distributed in a weighted manner to some of the unprocessed neighbour pixel. Each neighbour pixel value is adjusted by substracting the weighted errors made at the previous pixel locations. Finally these adjusted pixel values are thresholded in order to obtain the halftoned output. The error feedback that is introduced this way results in a representation of the average grey levels in the halftoned image that resembles the grey levels in the original image. It is noted that the fixed value of threshold level T only influences the run in behaviour of the error diffusion algorithm. The continuous tone input value is corrected with previously made errors until this corrected value reaches that of the fixed threshold, after which it will remain within a range with a maximum deviation to the threshold of one (255). A schematic view of the basic algorithm is shown in figure 3.14.

Floyd and Steinberg [Flo76] where the first to describe the properties of the error diffusion algorithm. The error diffusion mask that they propose is developed on a trial and error basis, but is still the smallest error diffusion mask available that produces good results and therefore is referred to as the standard error diffusion algorithm. The values of the standard error diffusion mask were chosen to assure the checkerboard pattern at middle grey.

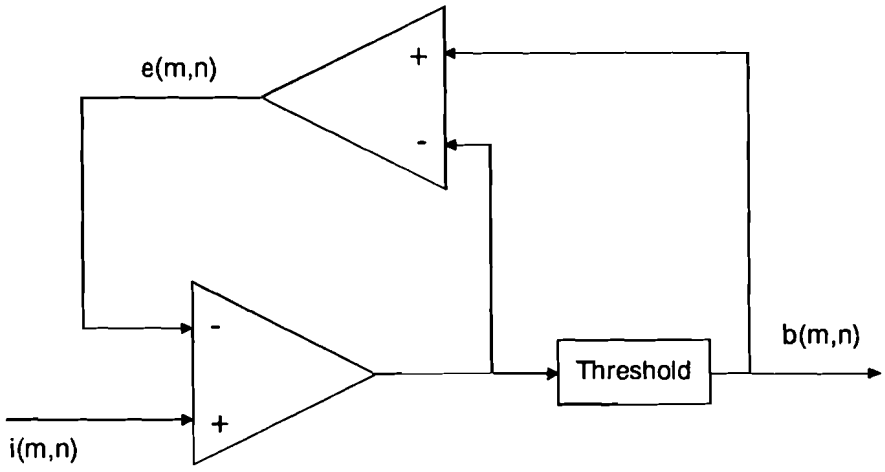

Figure 3.14: Schematic view of the basic error diffusion algorithm.

The Floyd and Steinberg error diffusion mask is depicted in figure 3.15.

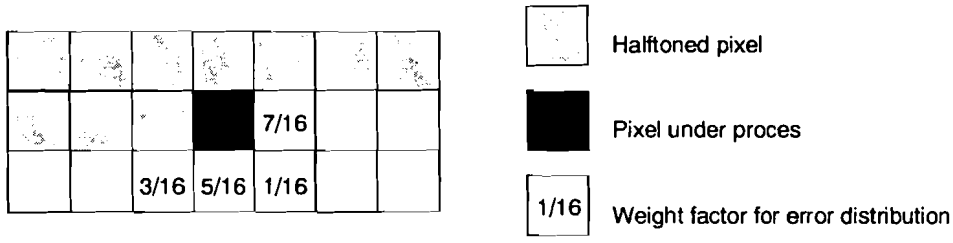

Figure 3.15: Floyd and Steinberg error diffusion mask.

An example of an image halftoned with the standard error diffusion algorithm is depicted in figure 3.16.

From figure 3.14 it follows that the error diffusion algorithm can be represented with the following equations

$$b(m,n) = step[i(m,n) - \sum_{j,k} a_{jk} e(m-j,n-k) - T], \tag{3.22}$$

and

$$e(m,n) = b(m,n) - [i(m,n) - \sum_{j,k} a_{jk} e(m-j,n-k)], \tag{3.23}$$

where $b(m,n)$ represents the halftoned output pixel at location (m,n),
$i(m,n)$ represents the input pixel at location (m,n),
$e(m,n)$ represents the produced error at location (m,n),
T equals the threshold (which is typically a constant of value 0.5) and
$a_{j,k}$ are the error distribution weights which distribute the error to locations j and k.

Figure 3.16: Example of an image halftoned with the standard error diffusion algorithm.

The step function in equation 3.22 is defined by

$$step(x) = \begin{cases} 0, & \text{for } x<0 \\ 1, & \text{for } x \geq 0 \end{cases}.$$

It is shown in equation 3.22 that the halftoned output at location (m,n) is determined by thresholding the modified input at (constant) threshold level T. Equation 3.23 shows that the error is determined from the difference between the halftoned output and the continuous-tone input modified with errors from previously processed pixels.

Since equation 3.22 is nonlinear it is hard to reduce further. Equation 3.23 is linear however, and can be simplified by using Fourier Transforms. The Fourier Transform of a function will be represented by its corresponding capital letter. Fourier transforming equation 3.23 results in

$$E(u,v) = B(u,v) - I(u,v) + \sum_{j,k} a_{jk} e^{-i(uj+vk)} E(u,v). \tag{3.24}$$

By rearranging the terms equation 3.24 can be written as

$$B(u,v) = I(u,v) + F(u,v) E(u,v) , \tag{3.25}$$

with

$$F(u,v) = 1 - \sum_{j,k} a_{jk} e^{-i(uj+vk)}. \tag{3.26}$$

Equation 3.25 shows that the properties of the halftoned image are different from the original image because a filtered version of the error screen is added to this input image. The filter *F(u,v)* is described by the weighing factors of the error distribution scheme. For the Floyd and Steinberg error diffusion mask the filter has asymmetric high-pass characteristics with a dc component that equals zero. This means that *B(0,0) = I(0,0)* and therefore the average values of the halftoned output image and the input grey-scale image are the same. Because of the high-pass nature of the filter only the high spatial frequency components of the error spectrum, *E(u,v)*, pass into the output spectrum, *B(u,v)*, which explains the edge enhancement and the blue noise characteristics of the error diffusion algorithm. Since these high frequency components are in general less visible to the human eye, a pleasing looking binary image is produced. In figure 3.17 plots of the modulus of the Floyd and Steinberg error diffusion filter are depicted.

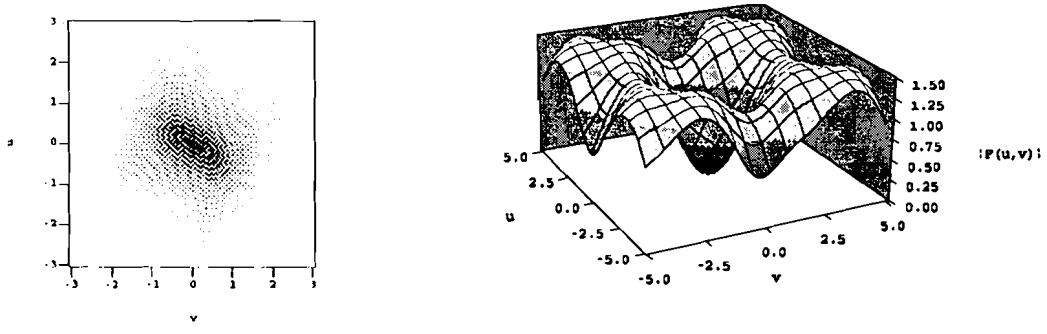

Figure 3.17: Modulus of the Floyd and Steinberg error diffusion filter.

To examine the edge enhancement properties of the error diffusion algorithm an image with background grey value 200 and in the middle a bar with grey value 50, is processed. By determining the ratio of black and white pixels as function of the *x*- or *y*-coordinate an impression of the edge enhancement properties is obtained. The normalized ratios, representing the grey values, obtained from an image with a vertical bar (horizontal edge) and an image with a horizontal bar (vertical edge) are depicted in figure 3.18 [a] and figure 3.18 [b], respectively. Figure 3.18 shows that the constant grey levels are reproduced well and that at the edges, especially for

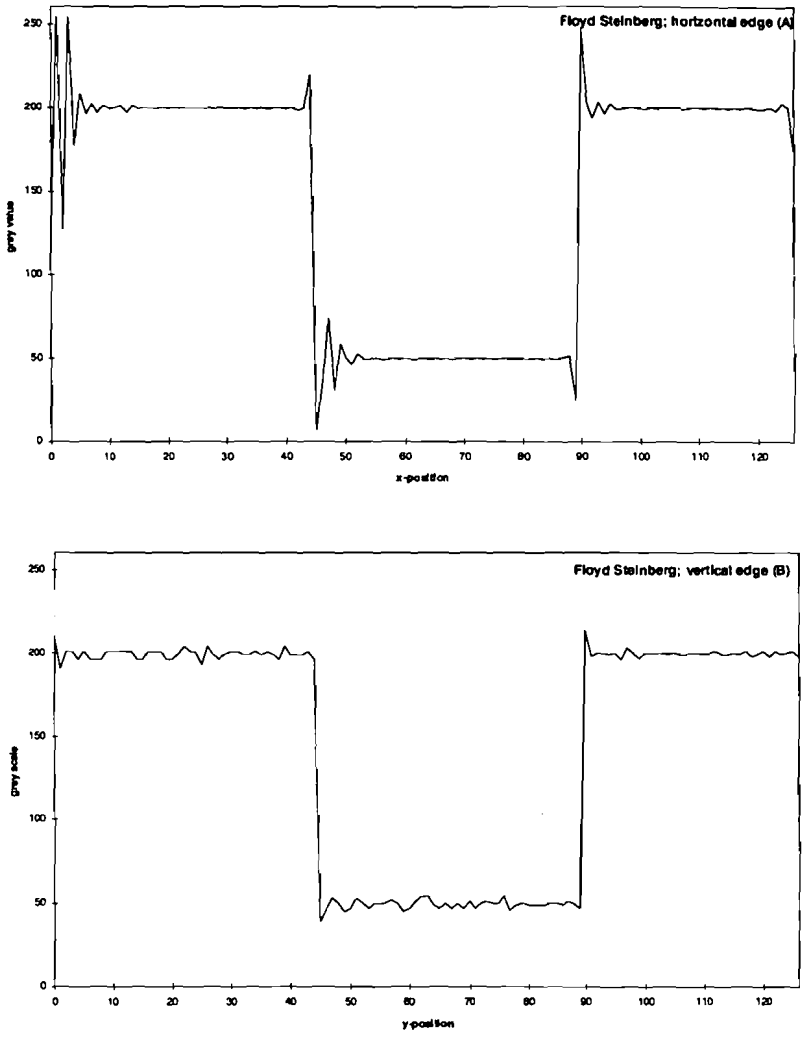

Figure 3.18: Edge enhancement properties of standard error diffusion on a horizontal edge (A) and a vertical edge (B).

the horizontal edge, an over- and undershoot occurs. The amount of over- and/ or undershoot represents the edge enhancement properties as well as the edge artifacts of the algorithm. From figure 3.18 it follows that the error diffusion algorithm is more sensitive for horizontal edges than for vertical edges, which becomes clear when the error diffusion mask is considered (see also figure 3.15). Taking into account the property of error diffusion to correct for the made errors as soon as possible, it follows from the error diffusion mask that a large amount of the made error, knowing $7/16^{th}$, is passed to the right neighbour pixel which will result in edge enhancement for especially horizontal edges. For vertical edges however, it follows that the made error at the pixel under process is diffused to three different neighbour pixels resulting in a less dominant edge enhancement effect. It is mentioned that the first and third spikes result mainly from the 'south-west' ($3/16^{th}$) error weight and that the second and fourth spikes result from the 'east/ south-east' ($7/16^{th}$ and $1/16^{th}$) error weight. The difference in the value of the error weights explains the difference in height of the spikes.

From figure 3.18 it is concluded that application of the error diffusion technique results in edge enhancement. It is mentioned that the spikes at the boundaries of figure 3.18[a] result from transient behaviour. These boundaries can in fact also be interpreted as sharp edges.

In order to show some of the properties of the error diffusion algorithm a grey scale ramp is processed and depicted in figure 3.19.

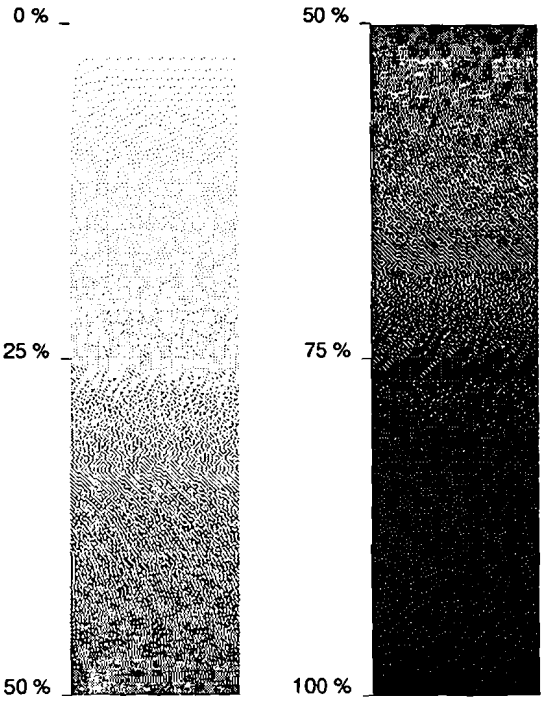

Figure 3.19: Grey scale ramp processed with standard error diffusion.

From figure 3.19 it becomes clear that most grey levels are represented by pleasing isotropic, structureless distributions of dots, which explains the popularity of error diffusion. On the other hand however, the grey scale ramp also shows some of the disadvantages of the error diffusion technique. It first of all becomes clear that error diffusion results in correlated artifacts in many of the grey values, especially in the 25%, 50% and 75% regions. This is explained by the fact that with error diffusion the complete error is distributed to the neighbourhood pixels. Since error diffusion is optimized to assure the 'checkerboard pattern' for a grey value of 50% it results in patterns with correlated artifacts for grey values of for instance about 50%. This happens because for these grey values a small error is distributed to the neighbourhood pixels. This error builds up until it is large enough to cause the 'broken checkerboard' patterns. Figure 3.20 shows some sensitive grey values for which the above mentioned artifact is clearly visible.

A second shortcoming of error diffusion is the occurrence of directional hysteresis, 'wormlike patterns', which are visible in the light and dark regions. See also figure 3.19. These structures can mathematically be characterized as anisotropy in the frequency spectrum of the resulting halftoned image [Uli87]. The direction of asymmetry in the error distribution filter, see also figure 3.17, determines the direction of these visually disturbing patterns. It is noted that the more the symmetry of the error distribution filter deviates from a circle symmetric form, the coarser the

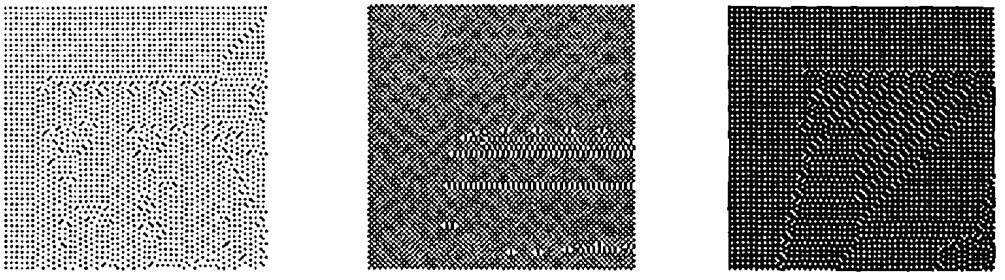

Figure 3.20: 'Sensitive' grey values processed with error diffusion, 26% (A), 51% (B) and 76% (C).

correlated artifacts will be and the more edge enhancement will be anisotropic. A third artifact of error diffusion is the transient behaviour near sharp edges or boundaries. This also results from the error distribution property of the algorithm.

In summary it is stated that error diffusion is a halftone technique that, opposed to traditional screening or ordered dither techniques, renders smoothly varying and high-frequency information, like edges, very well, results in halftoned images with exactly the same average grey level as the original input image and has the ability to reproduce an unlimited number of grey shades. It is noted however, that besides the artifacts mentioned above error diffusion also produces a lot of individual dots and very fine patterns from which a noisy impression in the halftoned output image can occur. This happens when the resolution of the printing device used is not high enough or when the resolution of the printing device is very high and therefore the individual dots can not reliably be printed. Form the performed experiments it can be concluded that standard error diffusion applied on a 400 dpi print engine will result in visually disturbing artifacts when smooth information needs to be rendered. Hence, higher resolutions which can reliably be reproduced are needed for application of the standard error diffusion algorithm.

At this point there are no methods known to men that give clear criteria in terms of visibility of undesirable image noise patterns, nor are there methods known to trade-off between image content and appearance of noise. Therefore most halftone design is, despite the state of the art in understanding of visual interpretation, still performed empirically. The fact that a halftone image from the point it leaves the pure digital world is affected by the messy real world of chemistry and physics, known as the printing process, which is not well modeled also, simply increases the uncertainty of mathematical prediction of output image quality.

Several techniques that try to eliminate some of the above mentioned artifacts are discussed in the next paragraph.

3.3.2 Modified error diffusion algorithms

Different techniques have been developed to eliminate the visual artifacts, like the wormlike and other correlated patterns, that occur when error diffusion is applied. Several modifications to the basic error diffusion algorithm will be discussed.

Choice of the error distribution mask

For the error diffusion algorithm a lot of different error distribution masks are possible. The distribution masks can consist of weights that vary in number, position and value. Figure 3.21 shows examples of some of the most occurring error distribution masks.

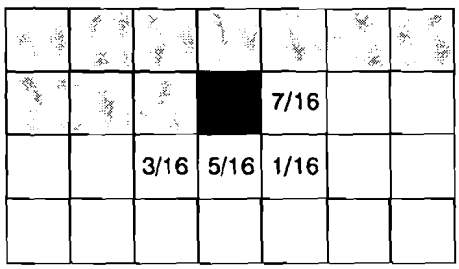

Floyd and Steinberg (1975)

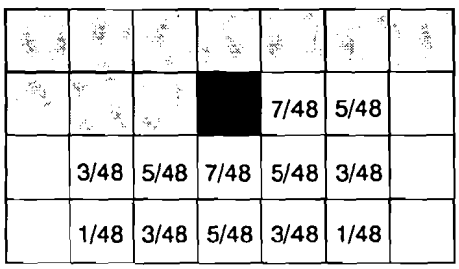

Jarvis, Judice and Ninke (1976)

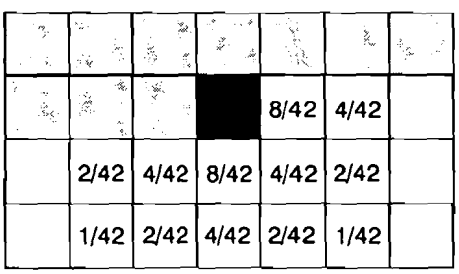

Stucki (1981)

Figure 3.21: Examples of error distribution masks.

It is obvious that for computational efficiency an error distribution mask that is as small as possible is preferred. On the other hand use of the larger error distribution masks decreases the structured patterns somewhat and enhances the edges, especially the mask proposed by Jarvis.

Threshold modification

One of the most powerful tools to eliminate the structured patterns that occur in standard error diffusion is threshold modulation. Threshold modulation means that the threshold is allowed to vary spatially. This means that the constant threshold $\bar{T}$ in equation 3.22 is replaced by the

function T - $t(m,n)$, with $t(m,n)$ the threshold function. The theoretical analysis of threshold modulation is described by Knox [Kno93[2]]. Knox introduces an equivalent input image, $i_e(m,n)$, that by definition results in the same halftoned output when processed with standard error diffusion as when the original input image, $i(m,n)$, is processed with the threshold modulated error diffusion algorithm. The spectrum of the equivalent input image can be written as

$$I_e(u,v) = I(u,v) + F(u,v)\,T(u,v), \tag{3.27}$$

where $I_e(m,n)$ represents the spectrum of the equivalent input image,
$I(m,n)$ represents the spectrum of the original input image,
$F(u,v)$ equals the standard error diffusion filter described earlier and
$T(u,v)$ is the Fourier Transform of the threshold modulation function $t(m,n)$.

The relationship in equation 3.27 is shown graphically in figure 3.22.

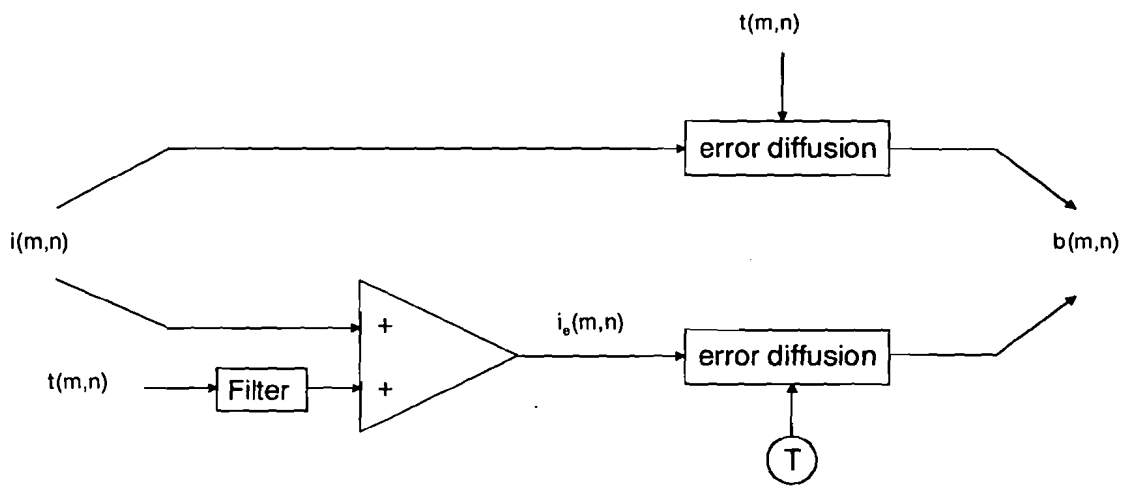

Figure 3.22: Modulation of the threshold in error diffusion is identical to processing an equivalent input with standard error diffusion.

It is obvious that the threshold can be modulated with many functions. In order to break up the unwanted patterns in the halftoned output image noise can be added to the threshold, i.e.

$$T(u,v) = cN(u,v), \tag{3.28}$$

where $N(u,v)$ equals the noise pattern and c is a constant.

Substitution of equation 3.28 in 3.27 results in

$$I_d(u,v) = I(u,v) + cF(u,v)N(u,v). \tag{3.29}$$

Equation 3.29 shows that only high-pass filtered noise is added to the input image before it is processed with the standard error diffusion algorithm. Because with threshold modulation only the high-frequency (less visible) components of the noise are added to the original image, the obtained results will be better than when noise is added directly to the input image and still contains the visible low frequency components.

If the input image is used as a threshold modulation function edge enhancement in the halftoned output image can be obtained. Figure 3.23 shows the necessary modifications to the standard error diffusion algorithm.

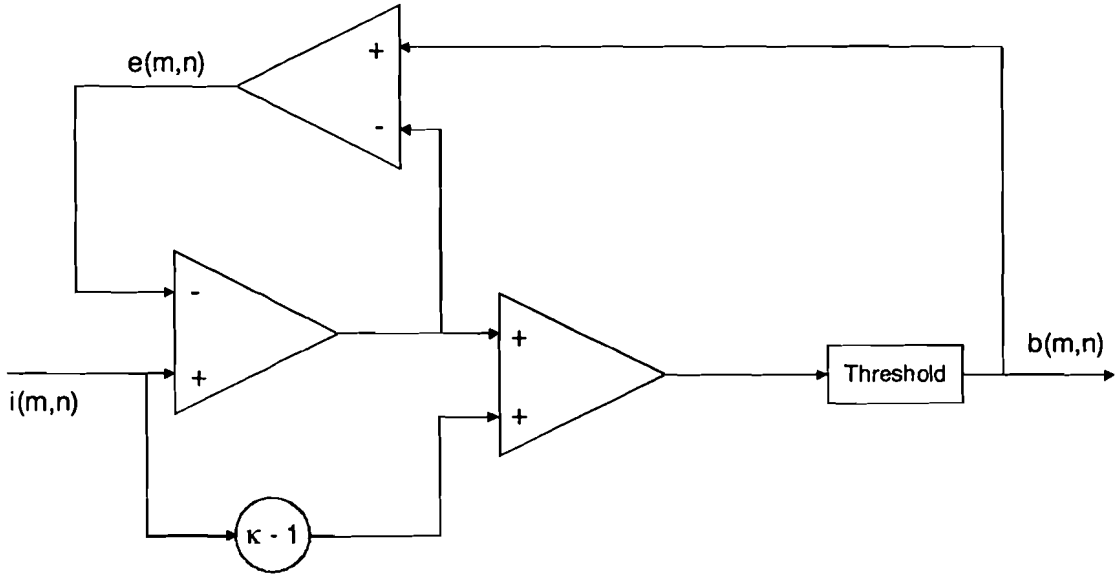

Figure 3.23: Modifications to the standard error diffusion algorithm in order to obtain edge enhancement.

The threshold spectrum can be written as

$$T(u,v) = (\kappa - 1)I(u,v), \tag{3.30}$$

with κ a constant that controls the amount of input image information that is included in the threshold modulation function. For the equivalent input image it follows that

$$I_d(u,v) = I(u,v) + (\kappa - 1)F(u,v)I(u,v). \tag{3.31}$$

Equation 3.31 shows that when $\kappa = 1$ the above algorithm equals the standard error diffusion algorithm. For $\kappa > 1$ a high-pass filtered version of the input image is added to the original input image before standard error diffusion is applied. This results in an edge enhanced halftoned

output image. The amount of edge enhancement is defined by κ. For $\kappa < 1$ the halftoned output image is blurred. Examples halftoned for different values of κ are depicted in figure 3.24.

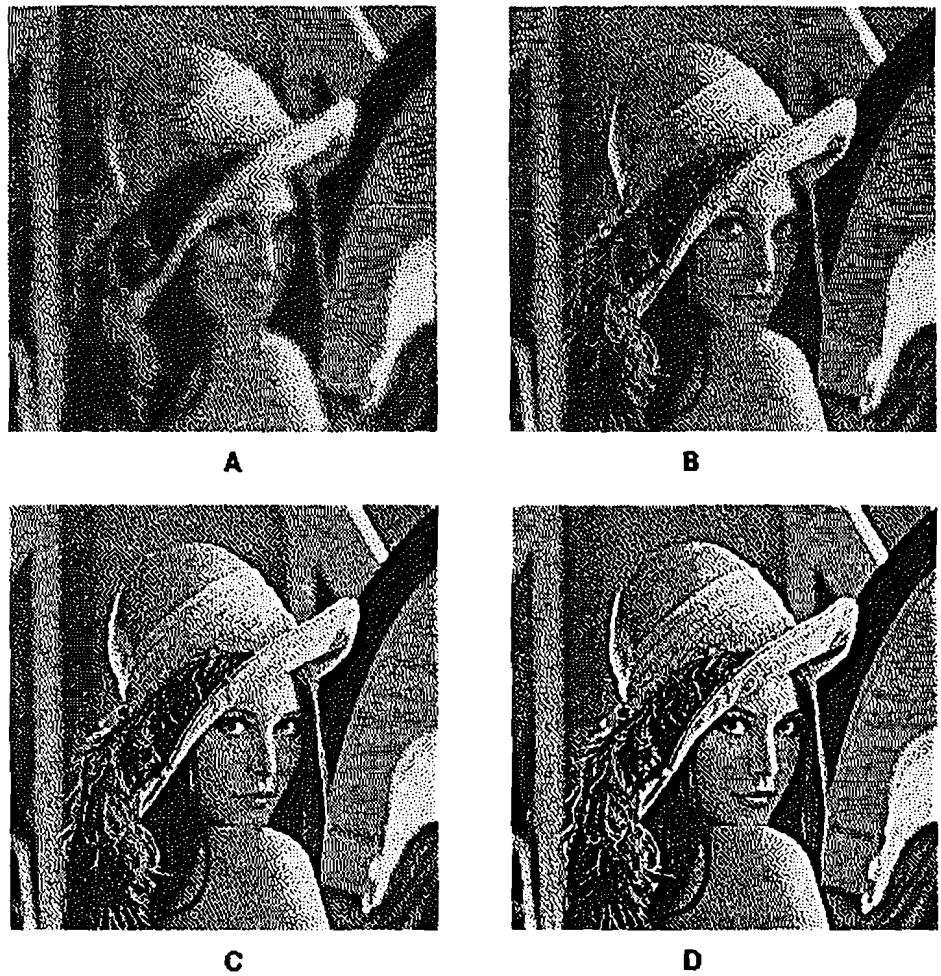

Figure 3.24: Error diffusion with the input image as threshold modulation function, (A) $\kappa = 0$, (B) $\kappa = 1$, (C) $\kappa = 2$ and (D) $\kappa = 3$.

Choice of the raster direction

Another way to eliminate the directional artifacts, obtained with error diffusion, are modifications that change the traditional raster order of processing the input image. Instead of processing the continuous tone image from top to bottom and each line from left to right many choices for space filling curves are possible. In literature examples of processing along a Hilbert or Peano curve (type of fractal) can be found. Also examples of error diffusion algorithms that process according to a randomized, space-filing curve can be found. A drawback of these techniques is that they impose heavy demands on memory.

In order to break up some of the wormlike patterns it is also possible to process according to a serpentine raster. This way a full two-dimensional buffer is not necessary and therefore the memory demands are less stringent. Figure 3.25[a] shows, together with a halftoned example, the

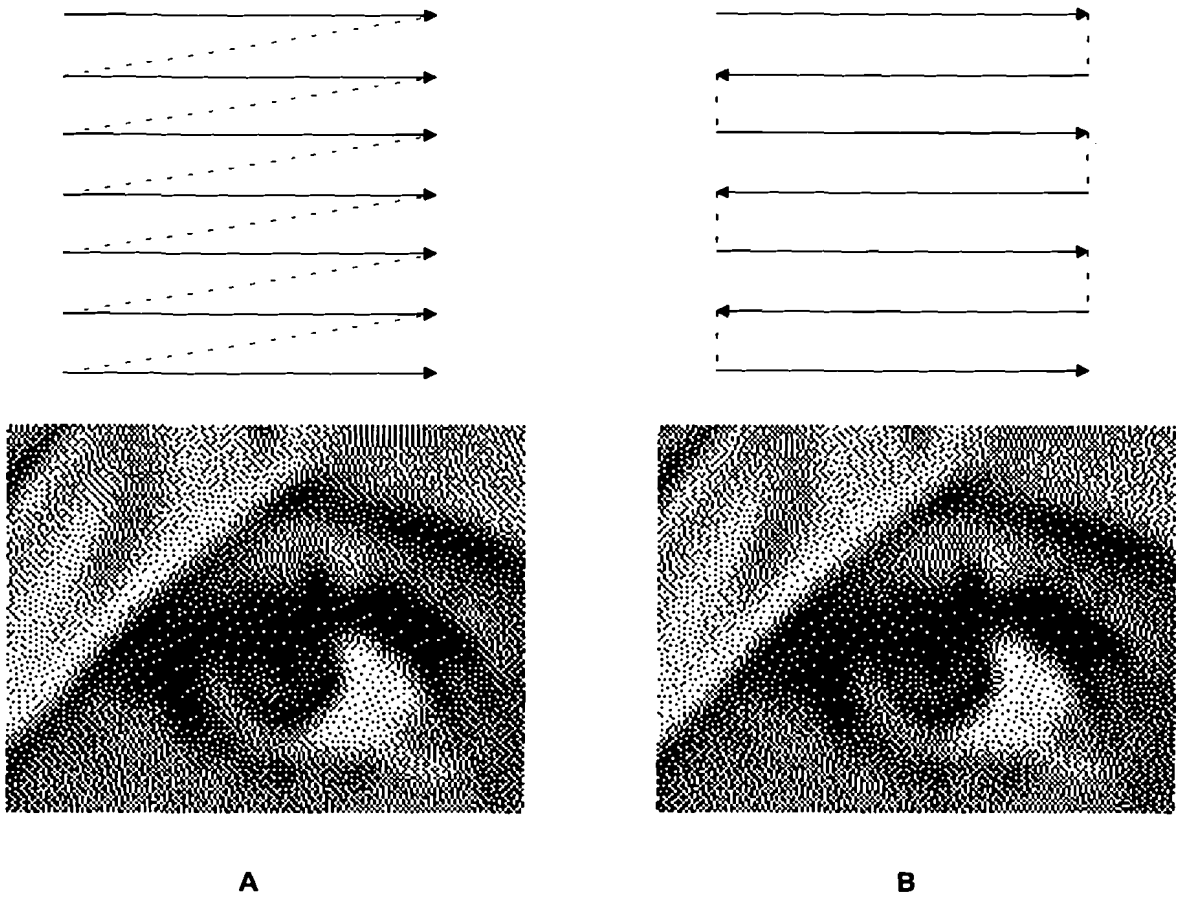

Figure 3.25: Example of a halftoned image when the traditional raster order (A) and when the serpentine raster order (B) is applied.

pattern that is followed when processing along the traditional raster is applied (see also figure 3.16). In figure 3.25[b] the processing path according to a serpentine raster is depicted. This reversal of processing means that the order in which the image pixels are processed and the direction in which the errors are passed (error distribution mask is mirrored for every new scanline), change between the odd and even scanlines. Knox [Kno93[1]] shows that when a serpentine raster is applied in combination with the standard error diffusion algorithm the Fourier Transform of the halftoned image can be split in a symmetric and asymmetric part. Because the symmetric part influences mainly the low frequency (visible) components and the asymmetric part the high frequency (non visible) components, use of the serpentine raster will result in less artifacts. A continuous-tone image processed with standard error diffusion along a serpentine raster is also shown in figure 3.25[b]. Figure 3.25[b] shows that some of the visually disturbing artifacts in the image processed along the traditional path, for instance the diagonal patterns in the upper left corner and the vertical bars in the upper right part of the image, can be eliminated when processing along a serpentine raster is applied. In figure 3.26 a grey scale ramp processed with error diffusion along a serpentine raster is depicted. It is mentioned that not all disturbing patterns are eliminated, but that especially in the very light and very dark parts of the grey ramp processing along a serpentine raster results in less correlated artifacts and therefore in better image quality.

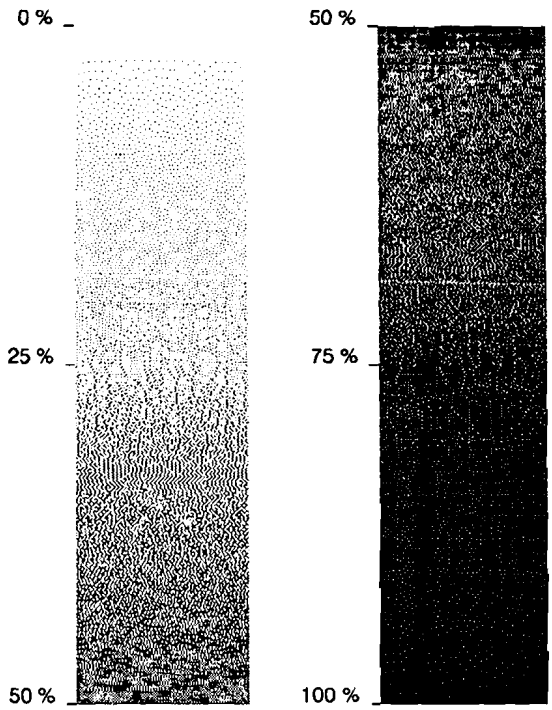

Figure 3.26: Grey scale ramp processed with standard error diffusion along a serpentine raster.

In order to examine the influence of processing along a serpentine raster on edge rendering the same experiments as for standard error diffusion (see paragraph 3.3.1) are performed. The normalized ratios, representing the grey scales, are plotted in figure 3.27[a] and figure 3.27[b] for a horizontal and a vertical edge, respectively.

When figure 3.27 is compared with figure 3.18 is becomes clear that processing along a serpentine raster has no consequences for the edge enhancement properties of the error diffusion technique. Because the error mask is reversed each line it follows that for horizontal edges processing along the serpentine raster results in 'symmetrical' edge enhancement, which is visualized by the symmetric distribution of the spikes in figure 3.27[a]. It is obvious that processing along a serpentine raster has practically no influence on vertical edges.

Stochastic perturbation of the error distribution mask

The structured patterns obtained with the standard error diffusion algorithm can also be prevented by adding noise to the weights in the error distribution mask. It is clear that the distributed error should equal the actual error made at the pixel location that is being processed, so the sum of the weights in the error distribution mask should always equal unity. This is realized by adding and substracting the same scaled random noise value to pairs of weights. This way it is guaranteed that the sum of the weights will always equal unity and therefore the grey scale impression of the continuous-tone image will be preserved in the halftoned image.

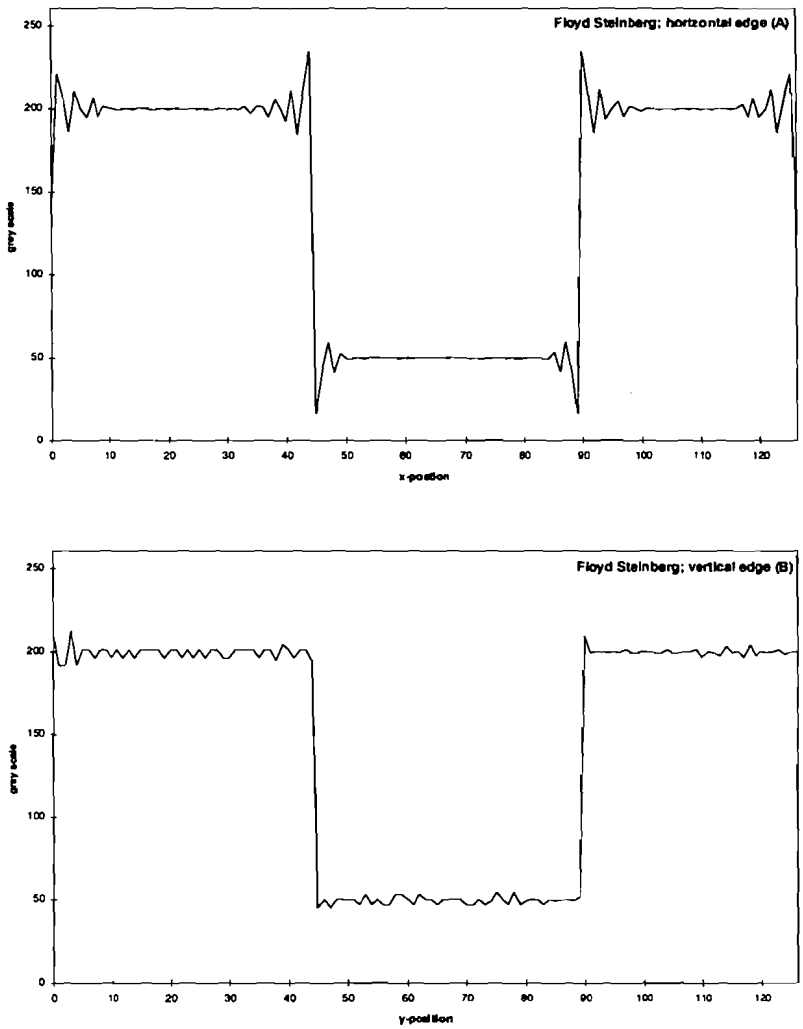

Figure 3.27: Edge enhancement properties of standard error diffusion processed along a serpentine raster, on a horizontal edge (A) and a vertical edge (B).

Besides randomizing the value of the weights in the error distribution mask also the positions of the weights can be randomized, with the constraint that the error must be distributed to unprocessed pixels only. This will also result in a decrease of the structured patterns in the halftoned images.

3.4 Classification of the key halftone techniques

The previous paragraphs describe the most commonly used halftone techniques. A classification of the different techniques is shown in table 3.1.

Table 3.1: Classification of the different halftone techniques.

	Screening		Ordered dither/ masking		Error diffusion	
	Clustered dot	Dispersed dot	Clustered dot	Dispersed dot	Clustered dot	Dispersed dot
Regular structures	Traditional screening		Clustered dot ordered dither			
Irregular structures				Bayer dither Void and cluster method Blue Noise masking	Error diffusion plus hysteresis Error diffusion with periodic threshold modulation	Error diffusion (perturbations in threshold, error filter and raster direction)

It is recognized that there are in principle three different halftone techniques that differ significantly from each other in the way they obtain the halftoned output image; screening, ordered dither techniques and error diffusion. Basically all the halftone techniques come down to an on or off decision based on a comparison of an input level with a threshold. Looking at the different techniques in this way they can in fact all be classified as dither techniques.

Each of the above mentioned techniques can be divided into methods that produce clustered or dispersed dot patterns. Clustered dot techniques try to group the individual dots in clusters, while dispersed dot techniques try to avoid clustering of individual dots.

Besides the different techniques a distinction is made in whether the halftone dots are arranged at regular or at irregular locations. Depending on the halftone technique used regular or irregular structures occur. Regular structures refer to rasters, fixed patterns, while irregular structures refer to more or less random structures. The irregular structures are preferred because of there visually pleasing patterns while the regular structures are preferred for there stability.

It follows from table 3.1 that in order to obtain printable irregular structures error diffusion with hysteresis or error diffusion with periodic threshold modulation might be promising techniques. Both techniques will be discussed in chapter 4 and chapter 5 respectively.

Chapter 4

Error diffusion with output dependent feedback

In chapter 3 it was concluded that in order to obtain visually pleasing halftoned images it is necessary to apply halftone techniques that produce irregular or more or less random structures. With error diffusion these visually pleasing patterns can be obtained and under the assumption of an ideal marking device, i.e. high resolutions and each addressable (sub)pixel can reliably be reproduced, application of this technique results in halftoned output images with the highest quality. In order to produce these high quality halftoned images most error diffusion techniques are optimized to produce halftone textures with energy predominantly in the very high spatial frequencies. This means that the halftoned images have blue noise characteristics which are very pleasing for the human eye.

In most situations however, the necessary reproduction conditions of marking devices, like printers, copiers and facsimile machines, are not as ideal as they should be. The extremely fine patterns resulting from the error diffusion algorithm can not reliably be reproduced, resulting in halftoned output images that obtain, especially in planes, a noisy impression. In this chapter a halftone technique, error diffusion with hysteresis [Lev91], is discussed, with which a coarser and therefore better reproducible and probably less noisy halftone output image can be obtained.

Hence, in order to produce images that can reliably be reproduced it is necessary to deliberately coarsen the halftone structures, thereby shifting the spatial frequencies from blue to green noise. This requires a technique that has the ability to vary the size of the dots used in producing the halftoned output image. By modulating the threshold with an output dependent feedback term, which equals the sum of the values of the two previously generated immediate neighbours of the pixel under consideration, these coarser halftone textures can be realized. The weight of this term is called the hysteresis constant h_x or h_y for the x and y direction respectively. The larger the hysteresis values h_x or h_y the coarser the resulting textures.

For reasons of clearness and simplicity the error diffusion with hysteresis technique is first explained by means of a one dimensional situation. Later the technique will be extended to a two dimensional situation.

4.1 Error diffusion with hysteresis in a one dimensional situation

It is supposed that *i(m)* represents the sampled input continuous tone value obtained by the scanning device ($0 \le i(m) \le 255$). *B(m)* is the output of the halftone algorithm, after thresholding the with previously made errors corrected input continuous tone value. The output *b(m)* of the halftone algorithm can be zero or one if the marking device is to produce a white or a black dot respectively. It is obvious that in order to maintain the important property of error diffusion, that the average error approaches zero, this output value needs to be scaled to the same dynamic range as the input value. This means that when *b(m)* equals zero or one the values zero and 255 respectively, will be used in calculations determining the errors made. The number and size of white and black dots needed to represent a given tone value is influenced by modulating the threshold with the previous output *b(m-1)*. The larger the weight of this output dependent feedback term, called the hysteresis factor, the larger the white and black dot will be. Since in this paragraph only the one dimensional situation is discussed an error made at location *m* will be completely passed to the next pixel at location *m+1*. This is shown in figure 4.1.

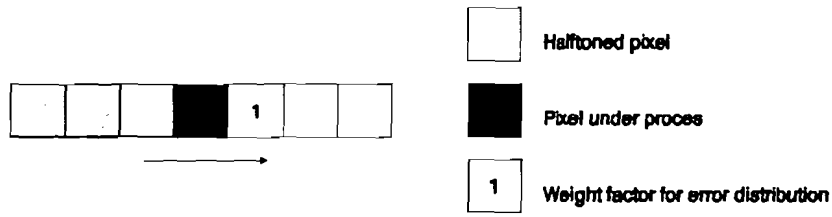

Figure 4.1: Error diffusion mask for the one dimensional situation.

For the one dimensional situation the halftoned output of the error diffusion with hysteresis algorithm is written as

$$b(m) = step[i(m) - e(m-1) - [T_0 - h.b(m-1)]] , \tag{4.1}$$

and

$$e(m) = b(m) - [i[m] - e[m-1]], \tag{4.2}$$

where *b(m)* represents the halftoned output at location *(m)*,
i(m) represents the sampled input continuous tone value at location *(m)*,
e(m) represents the calculated error at location *(m)*,
T_0 represents a fixed threshold and
h represents the hysteresis factor.

It is noted that the step function in equation 4.1 is defined by

$$step(x) = \begin{cases} 0, & for\ x<0 \\ 1, & for\ x \ge 0 \end{cases} . \tag{4.3}$$

From equation 4.1 it follows that when the previous output value, *b(m-1)*, equals one, the threshold T_0 is lowered with the hysteresis constant *h*. It is clear that because of this lower threshold it is now easier for the algorithm to produce an output value that equals one, thereby generating larger dots. On the other hand, when the previous output value equals zero the threshold is at its high value T_0 and therefore it is more difficult for the algorithm to produce the high output value. The above makes clear that because of this hysteresis factor the generated black and white dots become larger and the resulting halftoned output image will be easier to reproduce.

It can be shown that for the one dimensional situation the general form of equation 4.2 can be written as

$$e(m) = \sum_{j=0}^{m} (b(j) - i(j)). \tag{4.4}$$

If *e(m)* in equation 4.4 approaches zero the halftoned output image *b(m)* approximates the continuous tone input image *i(m)*. The hysteresis constant *h* however, defines an allowable excursion of the error around zero and therefore can be interpreted as the difference between the output and the input. Over a large number of points the average error, which is *e(m)* divided by the number of points, approximates zero. Hence, because of this hysteresis constant locally a relative large error is allowed in order to obtain larger dots and gain reproduction stability of the printing process. This error is corrected for over a larger part of the image thereby maintaining the average tone values of the continuous tone input image. Thus the output tone value is approximately equal to the input tone value.

Figure 4.2 illustrates the influence of the hysteresis constant *h*. The vertical axis represents the with previously made errors corrected input value, while the horizontal axis represents the processing direction of this one dimensional example. For clearness and simplicity all input and error values are normalized between 0 and 1 and a constant grey level *i(0)* is assumed. It follows from figure 4.2 that the with previously made errors corrected input value is represented as a ramp like curve around threshold levels T_0 and T_0 - *h*. The positive slope of the ramp like curve equals the input value *i(m)* and causes white dots to be generated as long as the with previously made errors corrected input value lies between the threshold levels T_0 and T_0 - *h*. Once this value reaches threshold T_0 the step function of equation 4.1 flips thereby changing the threshold to the value T_0 - *h*, and black dots are generated as long as the threshold value T_0 - *h* is not reached. The negative slope of the ramp like curve in figure 4.2 equals *i(m)* - *1*. It is noted that the slope of the ramp is a function of the input tone value. Hence, for a constant input value which lies exactly between white and solid-tone the positive and negative slopes are equal. For light tone values the positive slope decreases and more white output pixels will be needed to bridge the distance between the two threshold levels T_0 and T_0 - *h*. For dark tone values however, the positive slope increases so only a few white output pixels are needed to bridge the threshold gap, resulting, together with the low negative slope, in the desired dark tone value.

When figure 4.2 is considered the effect of changing the hysteresis constant *h* also becomes clear. If *h* is increased the threshold gap, which in fact is *h* itself, is increased. Because of this larger threshold gap more white and/ or coloured output pixels are needed to bridge the gap which will result in an increment of the size of the white and coloured dots produced. When the hysteresis constant *h* decreases the threshold gap decreases, resulting in less coarser patterns in the halftoned output image.

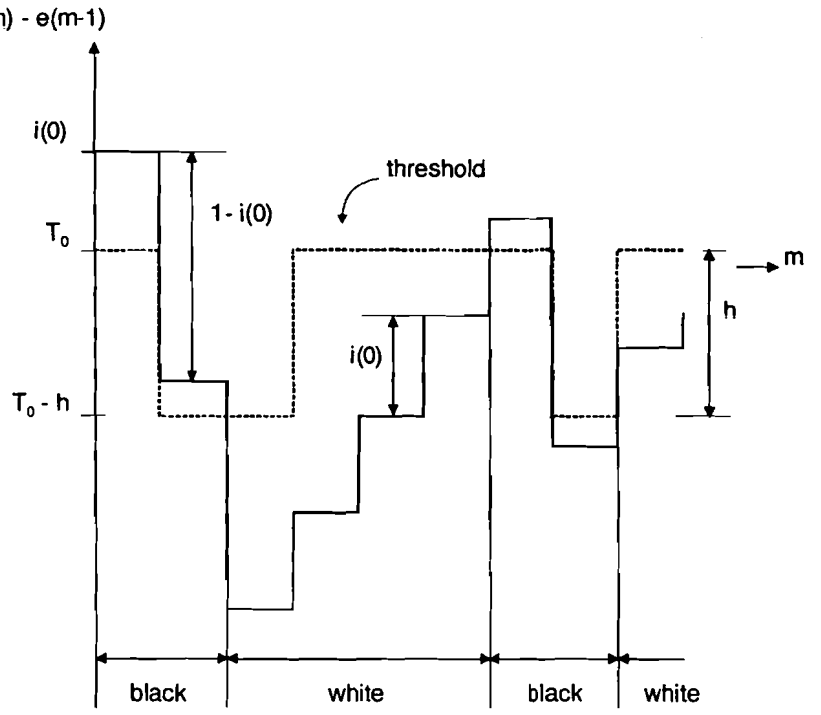

Figure 4.2: Effect of hysteresis constant *h*.

From the above it is concluded that, for a one dimensional situation and a constant tone value, the hysteresis constant *h* can be used to control the number of transitions from black to white and vice versa, thereby influencing the coarseness of the resulting halftoned output image. Hence, a high hysteresis constant will result in few transitions and therefore in a coarser better reproducible halftoned output image. In paragraph 4.2 the error diffusion with hysteresis algorithm will be expanded to a two dimensional situation.

4.2 Error diffusion with hysteresis in a two dimensional situation

In the previous paragraph it was shown that in a one dimensional situation, meaning one dimensional error distribution and a one dimensional scanning direction, the number of transitions from black to white or vice versa, which is equivalent with the coarseness of the resulting halftoned output image, can be controlled by influencing the weight of an output dependent feedback term. With this weight, called the hysteresis factor, a threshold gap can be controlled thereby influencing the size of the reproduced black and white dots.

In expanding the error diffusion with hysteresis algorithm to a typical two dimensional situation the scanning procedure and distribution of the error must be addressed. Different experiments are performed for the traditional and the serpentine raster scanning directions. Thus processing each line of the complete image from left to right as well as processing the even lines from left to right and the odd lines from right to left (see also figure 3.25) will be applied. For the distribution of the error the standard Floyd and Steinberg error diffusion mask will be used (see also figure 3.15). A schematic view of the two dimensional error diffusion algorithm with output dependent feedback is depicted in figure 4.3.

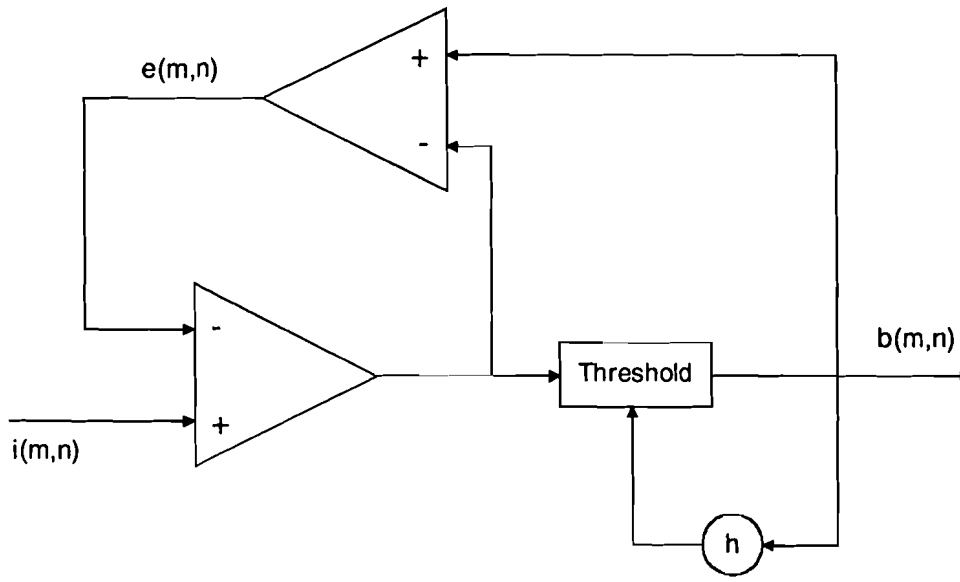

Figure 4.3: Schematic view of two dimensional error diffusion with output dependent feedback.

From figure 4.3 it follows that the error diffusion with output dependent feedback algorithm can be represented by the following equations

$$b(m,n) = step[i(m,n) - \sum_{j,k} a_{jk} e(m-j,n-k) - [T_0 - h_x b(m-1,n) - h_y b(m,n-1)]], \tag{4.5}$$

and

$$e(m,n) = b(m,n) - [i(m,n) - \sum_{j,k} a_{jk} e(m-j,n-k)], \tag{4.6}$$

where $b(m,n)$ represents the halftoned output at location (m,n),
$i(m,n)$ represents the sampled input continuous tone value at location (m,n),
$e(m,n)$ represents the calculated error at location (m,n),
T_0 represents a fixed threshold and
h_x and h_y are the hysteresis factors for respectively the x and y directions.

It is mentioned that for all necessary calculations the halftoned output value, $b(m,n)$, is scaled to the same dynamic range as the input value, $i(m,n)$, and the error, $e(m,n)$.

Experiments are performed for variation of the hysteresis factor in the tangential direction only, hence h_y will be used to coarsen the halftone patterns. This means that the threshold is only affected by the output value of the pixel that is directly above the pixel under process (h_x equals zero). Figure 4.4 shows a picture processed, along the traditional raster, with error diffusion and with different weights of the output feedback term.

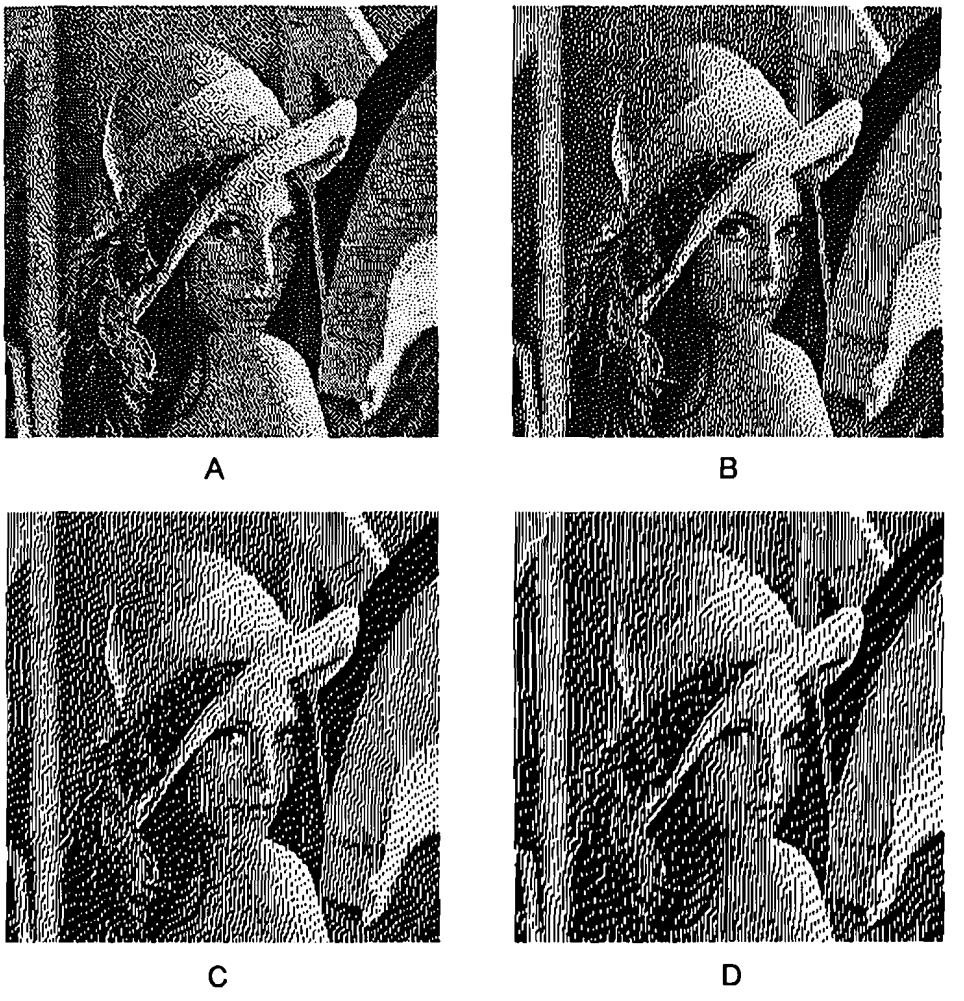

Figure 4.4: Error diffusion with hysteresis processed along a traditional raster, (A) $h_y = 0$, (B) $h_y = 0.25$, (C) $h_y = 0.50$ and (D) $h_y = 0.75$.

Figure 4.4 clearly shows that when the hysteresis factor increases the clustering of black and white dots in the vertical direction gets stronger, resulting in better reproducible but also visually more disturbing halftoned output images. Hence, by increasing h_y the resulting halftoned output image obtains more vertically correlated patterns. That the correlated textures in the halftoned output image are not only perfect vertical patterns is caused by the two dimensional distribution of the error and the asymmetrical form of the error distribution filter (see also figure 3.17). In figure 4.5 the same image is processed also with error diffusion for different hysteresis factors,

but now along a serpentine raster in order to try to eliminate some of the directional hysteresis caused by the error distribution filter.

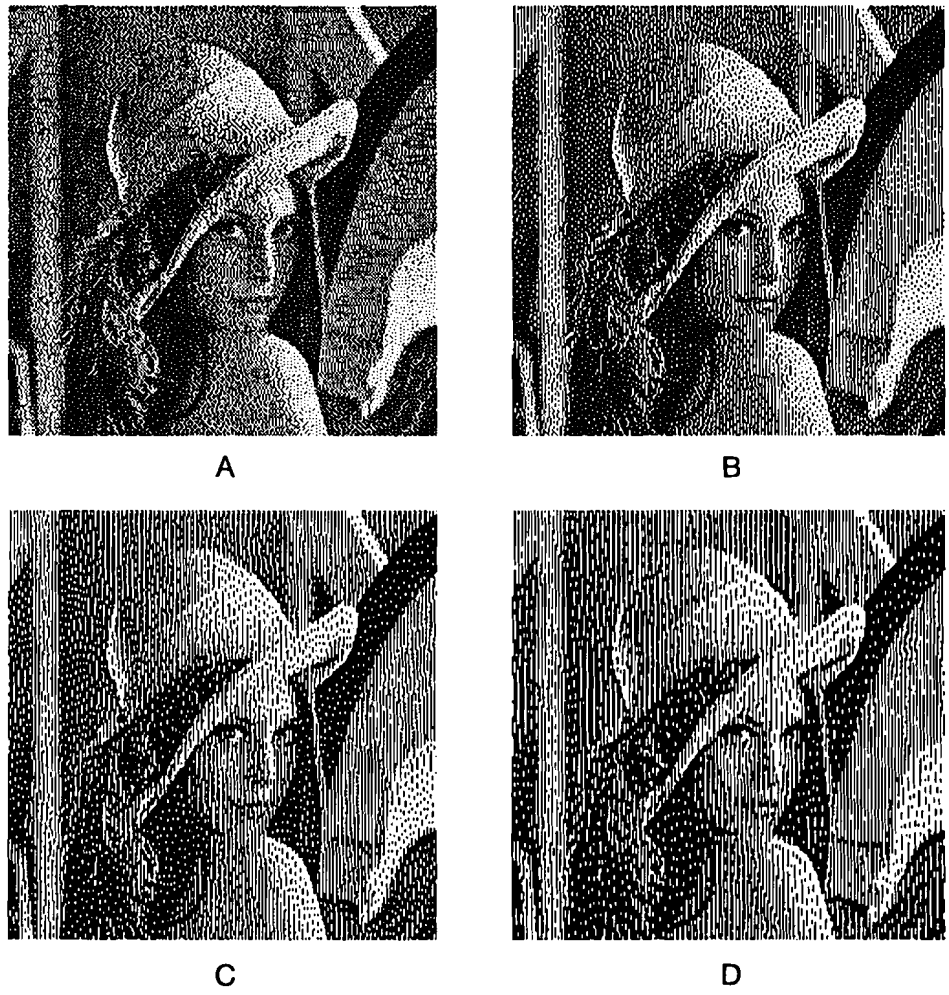

Figure 4.5: Error diffusion with hysteresis processed along a serpentine raster, (A) h_y = 0, (B) h_y = 0.25, (C) h_y = 0.50 and (D) h_y = 0.75.

It is shown in figure 4.5 that some of the unwanted directional hysteresis can be eliminated by processing along a serpentine raster. It is mentioned however, that although the image is processed along the serpentine raster some unwanted directional hysteresis still exists. The same can be concluded from figure 4.6[a] and 4.6[b] in which a grey scale ramp is processed, with hysteresis factor 0.50, along the traditional and the serpentine raster, respectively.

To examine the influence of hysteresis on the edge enhancement properties of the error diffusion algorithm the same experiments as in paragraph 3.3.1 were performed. A horizontal and vertical edge were processed with error diffusion along the traditional raster, with hysteresis factor 0.5. The normalized ratios representing the grey scales are plotted in figure 4.7[a] and 4.7[b] for the horizontal and vertical edge, respectively.

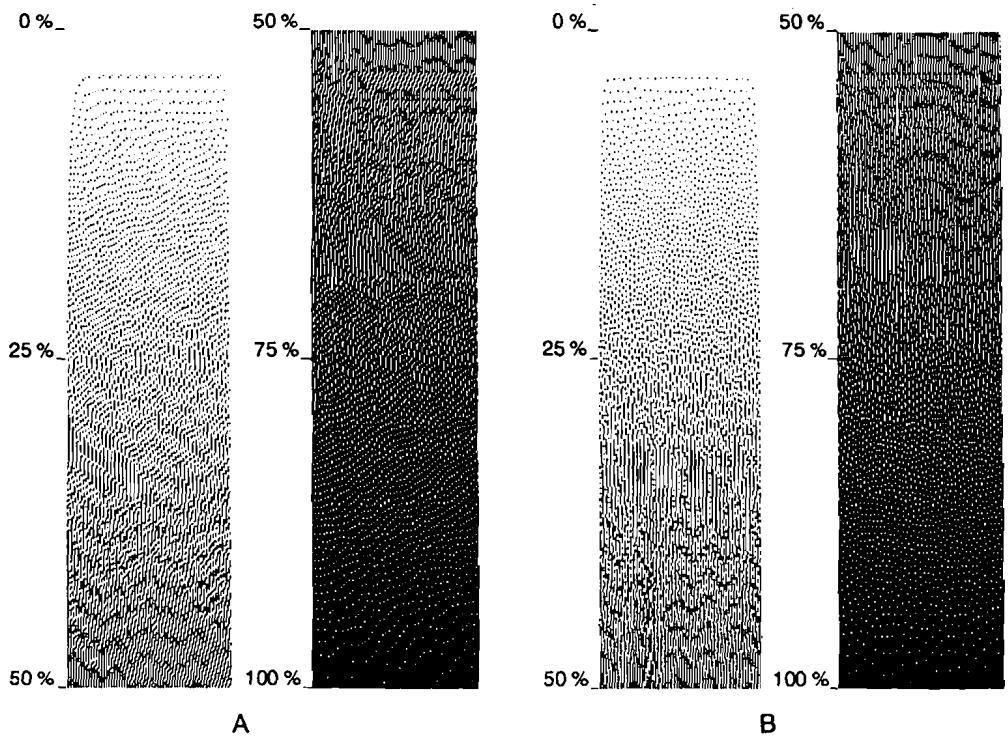

Figure 4.6: Grey scale ramp processed with error diffusion with hysteresis factor 0.5, along the traditional (A) and the serpentine (B) raster.

When compared with the standard error diffusion algorithm, see figure 3.18[a], figure 4.7[a] shows a larger amount of over- and undershoot, meaning better rendering of horizontal edges. From figure 4.7[b] it becomes clear that for the tone values and hysteresis factor applied, vertical edges are rendered just as good as when standard error diffusion is applied (see also figure 3.18[b]). It is noted however, that when the hysteresis factor becomes larger the edge starts 'moving' a few pixel locations, which is caused by the fact that by means of the hysteresis term the algorithm tries to maintain the output of the previous line. This effect is however only clearly noticeable for very large hysteresis factors like 3 or 5. For these high hysteresis values the textures in the output image are already visually very disturbing, resulting in poor image quality. It is therefore concluded that the vertical textures which result from the hysteresis term are visually more disturbing for rendering of vertical edges then for rendering of horizontal edges.

From figure 4.7 it is concluded that hysteresis in a direction perpendicular to an edge results in better edge rendering and therefore more edge enhancement. For edges in the same direction as the hysteresis component, the resulting patterns will visually be more objectionable which imposes application of only relative small hysteresis factors.

When processing according to a serpentine raster is applied, directional artifacts are slightly less and more symmetric edge rendering takes place (see also figure 3.27), but overall the same conclusions as for processing along the traditional raster can be drawn.

When figure 4.4 and 4.5 are considered it becomes clear that for a higher hysteresis factor the

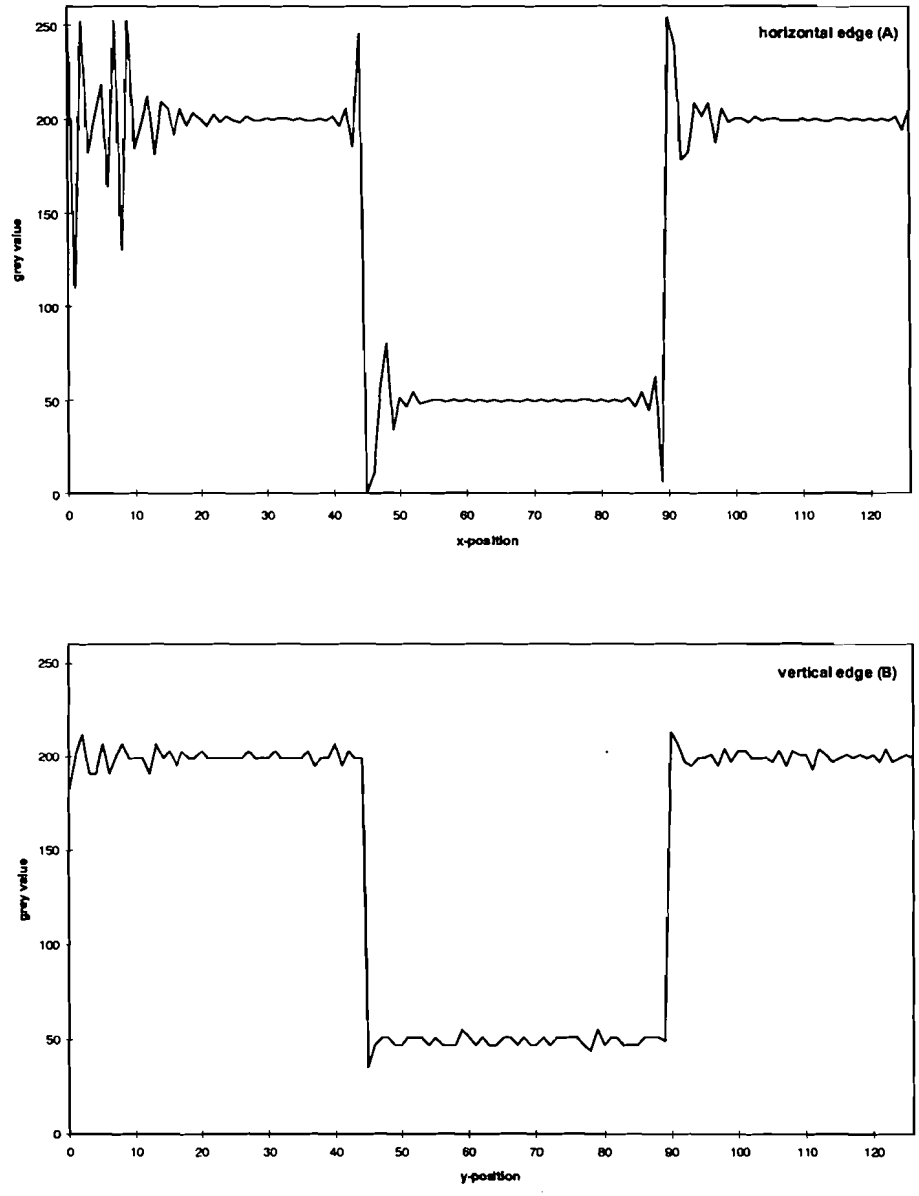

Figure 4.7: Edge enhancement properties of error diffusion with hysteresis, $h_y = 0.5$, for a horizontal (A) and a vertical edge (B) processed along the traditional raster.

resulting halftoned output image gets coarser, thereby obtaining better reproducible output images. When the hysteresis factor is too large the resulting textures get too coarse resulting in very visible and disturbing artifacts. On the other hand, when the hysteresis factor is too small the halftoned output image is not coarse enough, resulting in noisy and badly reproducible output images. Hence, an optimum for the hysteresis factor needs to be found.

By taking into account test-charts in which all possible combinations of subpixel clusters are

printed, it is presumed that for black a minimum runlength of two subpixels and for all other mono colours a minimum runlength of four subpixels is needed in order to be able to assure that the subpixel patterns addressed also get on paper. In order to determine the optimum value for the hysteresis factor which guarantees the above mentioned runlengths, planes with different constant tone values are processed for different hysteresis factors. From the resulting halftoned images the average runlength of the 'on' clusters, i.e. the average size, in the direction of the hysteresis component, of the dots that compose the tone value, is determined. In figure 4.8 this average runlength is depicted as function of the tone value and hysteresis factor.

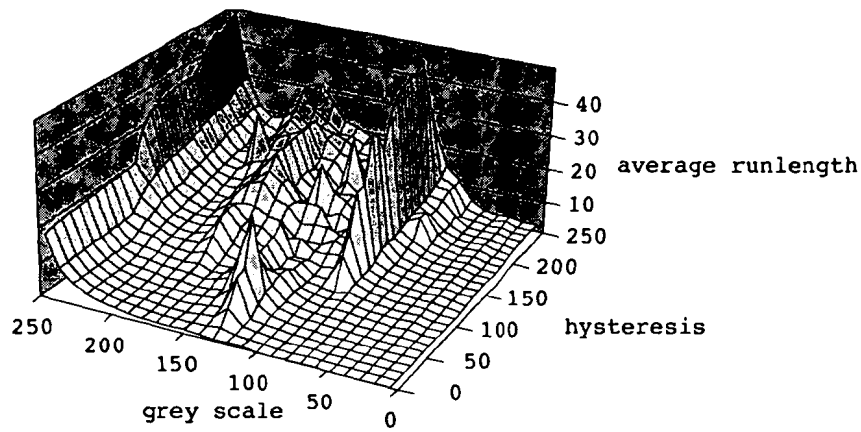

Figure 4.8: Average subpixel runlength as function of the tone value and hysteresis factor.

In figure 4.9 cuts of the average runlength as function of the grey value and as function of the hysteresis component are depicted. From figure 4.9[a] it becomes clear that for a constant hysteresis factor the runlength as function of the grey value does not increase monotonous. This means that many of the dark grey values are represented by shorter runlengths than some of the lighter grey values, which are represented by a few long runlengths. So in order to obtain the presumed stability, i.e. runlength, for some grey values a relative high hysteresis factor is needed, which will on the other hand result for some lighter grey levels in unacceptable long runlengths. It is obvious that this will result in very visible disturbing artifacts. Figure 4.9[b] shows that the average runlength as function of the hysteresis factor does not increase monotonous also. So increment of the hysteresis factor does not automatically mean longer average runlengths. This is caused by the fact that the error diffusion with hysteresis algorithm generates besides long runlengths also very short runlengths for some increased hysteresis factors, thereby decreasing the average runlength and generating patterns that are very difficult to reproduce reliably.

From figure 4.8 and 4.9 it is concluded that the error diffusion with output dependent feedback algorithm does not offer the possibility to produce halftoned output images with the desired reproducibility and high quality. The instability of the algorithm, caused by the two dimensional error distribution, makes it too hard to reliably control the generated output in order to guarantee the presumed runlengths and the related reproducibility of the halftoned output images.

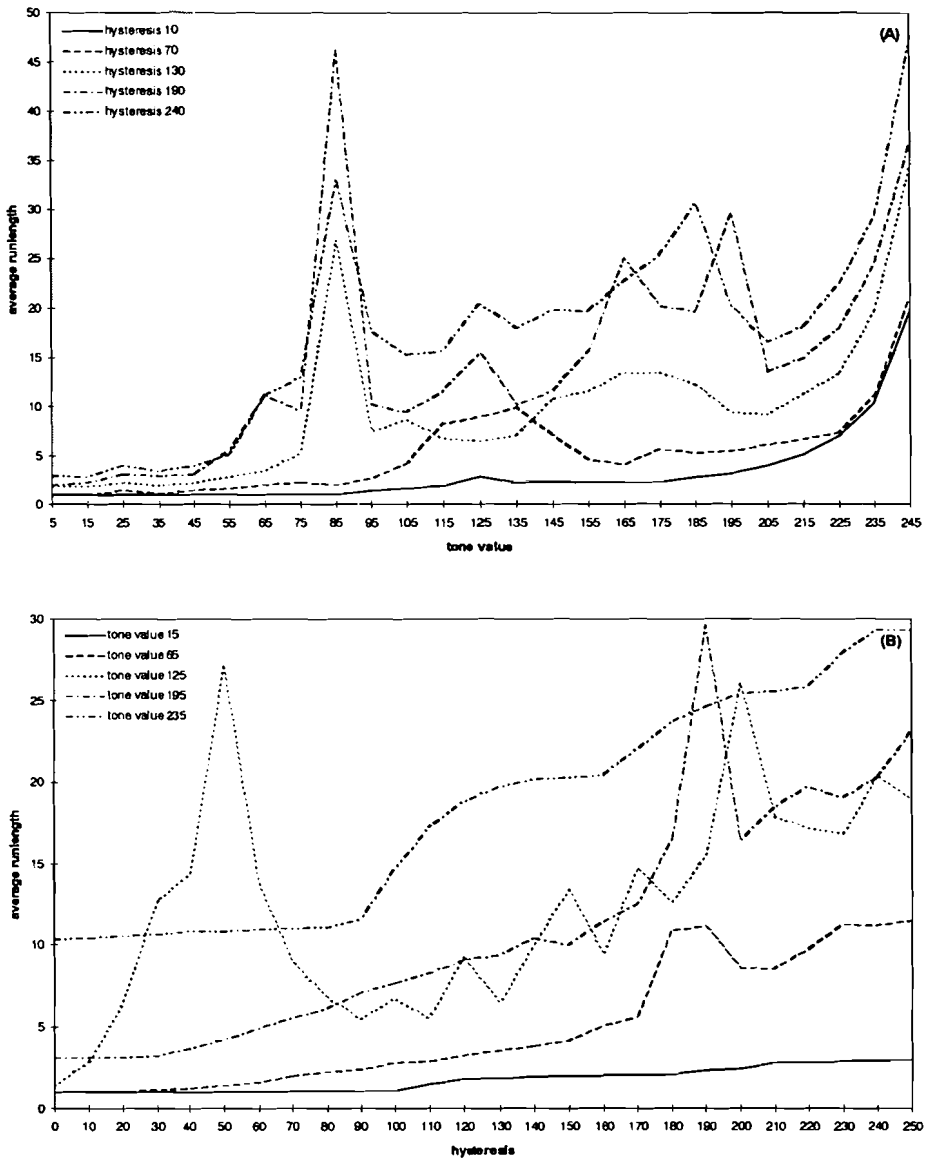

Figure 4.9: Average runlength as function of the tone vale (A) and as function of the hysteresis factor (B).

It is mentioned that experiments with alternative error diffusion masks, for example masks with negative error diffusion weights, were also performed. These negative weights are necessary in order to preserve a total error distribution factor of one, while at the same time an error weight already equals one in order to improve the controllability of the algorithm (see paragraph 4.1). Although application of these error diffusion masks increase the controllability with respect to the generated average runlengths (see figure 4.11), the form of the frequency spectrum of the resulting error diffusion filters differ a lot from the circle symmetric form of an ideal filter. Therefore application of these filters result in unwanted directional artifacts. An example of an

error diffusion mask with negative weights is shown in figure 4.10.

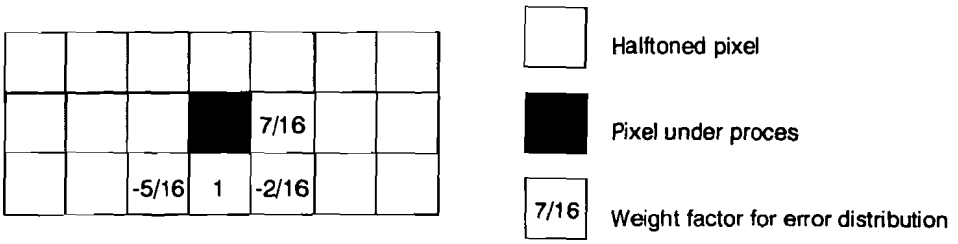

Figure 4.10: Alternative error diffusion mask.

In figure 4.11 the average runlength as function of the tone value and the hysteresis factor is depicted. The smooth path of the average runlength as function of grey values and hysteresis factors indicate improved controllability.

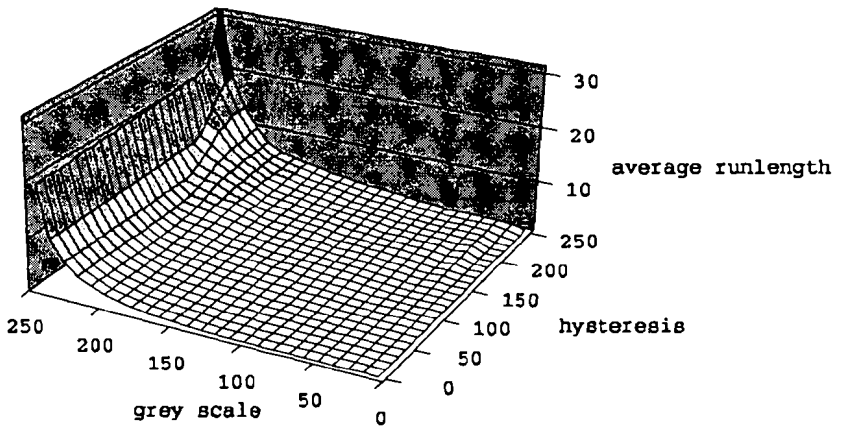

Figure 4.11: Average subpixel runlength as function of tone value and hysteresis factor.

Figure 4.12 however, clearly shows the asymmetric form of the modulus of the resulting error diffusion filter, which will result in visually disturbing artifacts, like coarse and unwanted correlated patterns and anisotropic edge enhancement.

4.3 Conclusions

In order to produce halftoned output images which contain the visually pleasing properties of the error diffusion algorithm and also can reliably be reproduced, error diffusion with output dependent feedback was examined. From the performed experiments it is concluded that the noisy impression that occurs when pure error diffusion is applied to areas with an almost constant tone value (planes) can not, with the output feedback loop, be eliminated without introducing other visually disturbing artifacts. The instability of the error diffusion with hysteresis algorithm makes it impossible to optimize this technique to a situation in which the resulting output image contains almost only the presumed minimum runlengths, thereby resulting in reproducible halftoned output images of optimum quality. Another important problem with

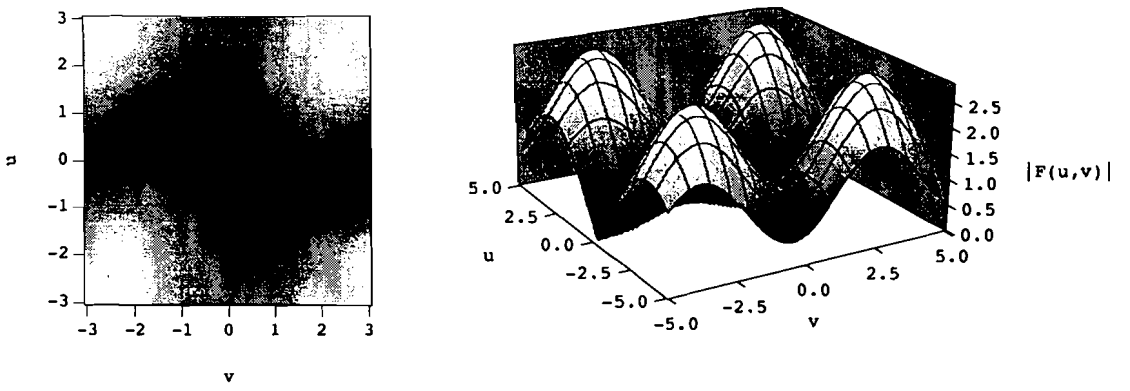

Figure 4.12: Modulus of alternative error diffusion filter.

hysteresis is that because of the vertical textures that arise from this technique the different separations become more sensitive to positioning errors in axial direction. This makes reliable and artifact free colour mixing next to impossible. Hence, in general it is concluded that the irregular and therefore hard reproducible textures of the error diffusion algorithm can not be eliminated by adding an output dependent feedback term to the algorithm, while maintaining high image quality. The resulting halftoned output image either contains stable, but visually disturbing patterns or still contains textures that are very hard to reproduce, which still results in a noisy impression of the halftoned output image.

Another conclusion that automatically follows from the above conclusions is that the resolution and reproducibility of addressed (sub)pixels are not high enough to apply pure error diffusion and obtain the high quality halftoned output images that error diffusion has in prospect. Hence, first when the resolution and reproducibility of (sub)pixels is improved pure error diffusion might be a promising technique in colour halftoning.

A technique that contains the stability and reproducibility of ordered dither techniques but also contains the edge enhancement properties of error diffusion will be discussed in chapter 5.

Chapter 5

Error diffusion with periodic threshold modulation

In order to change some of the characteristics of standard error diffusion several modifications have been discussed in chapter 3. Modulation of the error diffusion threshold with an output dependent feedback term, is discussed in chapter 4. It was concluded that addition of an output dependent feedback term did not offer the possibility to eliminate the noisy impression resulting in images halftoned with pure error diffusion. Although better printable patterns were created, other visible artifacts occurred resulting in deterioration of the reproduced image quality. Since especially the detail and edge rendering properties of error diffusion are very promising a technique that eliminates the noisy impression, which mainly occurs in smooth planes, needs to be found. Error diffusion with periodic threshold modulation offers the stability of ordered dither techniques, needed to eliminate the noisy impression resulting from the fine patterns created by the error diffusion algorithm and limitations of the print engine.

5.1 Basic algorithm

In order to use the error diffusion technique on copy and/ or print devices that require a clustered dot appearance to be able to consistently reproduce high quality haftoned output images, modifications to the standard algorithm are needed. Normally the standard error diffusion algorithm represents the continuous tone images by a dispersed set of dots. This dispersed dot property of error diffusion results in halftoned output images with blue noise characteristics, which are very pleasing to the human eye. Because of the high frequency properties application of standard error diffusion also results in high quality edge and detail rendering. See also paragraph 3.3. On the other hand however, these dispersed dot structures result in patterns that are highly unstable for reproduction on most devices, resulting, especially in smooth planes, in a noisy impression. It is mainly therefore that there is a continuing use of the standard clustered dot halftoning techniques, like ordered dither (see also paragraph 3.2.1), in copying and/ or printing applications.

This chapter deals with a modified standard error diffusion algorithm, called error diffusion with periodic threshold modulation, that tries to eliminate the noisy impression, by threshold variations resulting in clustered bi-level output dots similar to the output patterns obtained when standard clustered dot ordered dither techniques are applied. It is mentioned that in contrast to these standard ordered dither techniques the trade-off between the screen frequency and the number of tone values that can be represented in the resulting halftoned output image is alleviated. A

schematic view of the error diffusion with periodic threshold modulation technique is shown in figure 5.1.

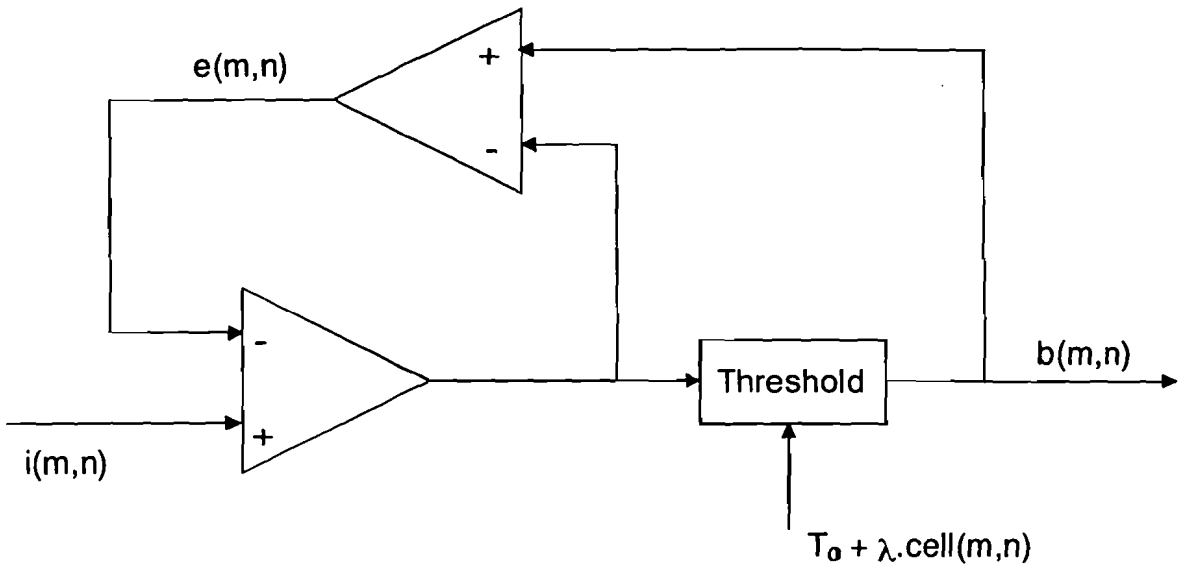

Figure 5.1: schematic view of error diffusion with periodic threshold modulation.

From figure 5.1 it follows that in order to generate a standard clustered dot or raster in the halftoned output image the threshold is modulated with the thresholds in a periodically varying dither cell [Esc94]. The halftoned binary output and the calculated error for the periodic threshold modulation algorithm is given by

$$b(m,n) = step[i(m,n) - \sum_{j,k} a_{jk} e(m-j,n-k) - [T_0 + \lambda cell(m,n)]], \tag{5.1}$$

and

$$e(m,n) = b(m,n) - [i(m,n) - \sum_{j,k} a_{jk} e(m-j,n-k)], \tag{5.2}$$

where *i(m,n)* represents the input continuous tonevalue at location *(m,n)*,
e(m,n) represents the calculated error at location *(m,n)*,
b(m,n) represents the halftoned output at location *(m,n)*,
$a_{j,k}$ are the error distribution weights which distribute the error to locations *j* and *k*,
T_0 represents a fixed threshold,
λ represents a multiplier and
cell(m,n) represents different threshold matrices.

The dynamic range of the thresholds in the dither matrices can be influenced by the constant multiplier λ. It is mentioned that when λ equals zero the algorithm is identical to standard error diffusion. In figure 5.2 a part of a continuous tone image, processed according to the error

diffusion with periodic threshold modulation algorithm, is depicted for different multiplication factors λ.

A

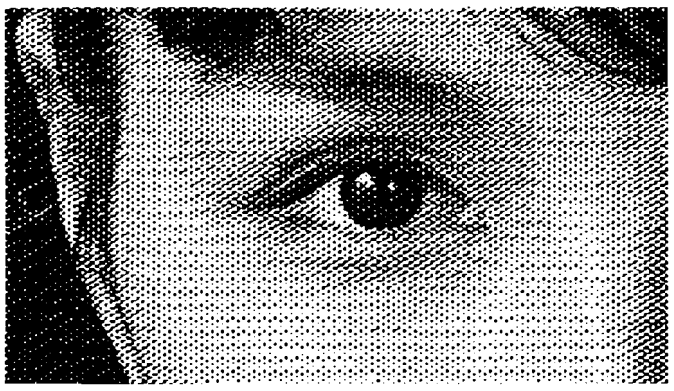

B

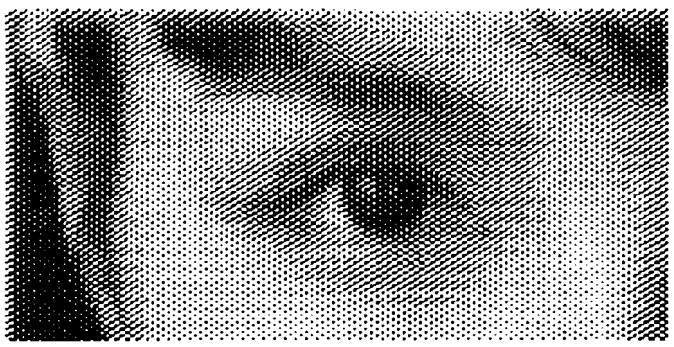

C

Figure 5.2: Error diffusion with periodic threshold modulation with λ = 0 (A), λ = 1 (B) and λ = 8 (C).

In figure 5.2 it is clearly visible that when λ is increased the individual dots get more and more clustered according to the patterns imposed by the dither matrices. As λ increases the error diffusion properties of the algorithm will finally be overruled by the dither cell and therefore the algorithm will more and more behave like the in chapter 3 discussed clustered dot ordered dither

technique. Obviously this will result in more stable and better reproducible halftoned output patterns. So, by modulating the threshold with a dither matrix with a large dynamic range the individual dots resulting from standard error diffusion can be clustered. The size of the chosen dither matrix determines the coarseness of the raster (see also paragraph 5.2).

From figure 5.2 immediately a major drawback of threshold modulation with a dither matrix becomes clear. As λ increases the individual dots get clustered but as a result the halftoned output image lacks sharpness and gets blurred. Because of the (necessary) large dynamic range of the dither cell, resulting from the large λ, all local variations in the input image are overruled resulting in the blurred halftoned output image. The disadvantage of small amplitude threshold modulation lies in the fact that the error diffusion algorithm behaves like an integrator and therefore small changes in the thresholds or decision levels are immediately compensated for by the error feedback. It is the large dynamic range variation of the thresholds, obtained by large λ's, that locally overrides the error diffusion effects and therefore allows an effective influence on the resulting output patterns, necessary to obtain good reproducible images.

Clearly something needs to be done about the edge and detail rendering in the above algorithm, but first some important remarks about the choice of the dither matrices used will be made in paragraph 5.2

5.2 Choice of the dither matrices

In order to obtain high quality rendering of smooth planes it is necessary to apply clustered dot ordered dither techniques or techniques which result in similar patterns. By modulating the threshold used in error diffusion with a dither matrix, these stable and therefore good reproducible output patterns can be obtained. The choice of the dither matrix used is a compromise between screen visibility, number of tone values that need to be represented, micro-smoothness, moiré and print engine properties.

As was mentioned in chapter 2, each colour separation needs to be halftoned and the resulting output must be as independent as possible from all other halftoned separations in order to avoid moiré. Since with clustered dot ordered dither techniques the resulting output patterns obtain regular structures, interference between different halftoned separations can easily occur, resulting in visually disturbing moiré phenomena.

An important engine property that influences the choice of the dither matrices a great deal is the accuracy and stability with which the different separations can be positioned on the central intermediate. If this is not done very accurately, colour-shifts as well as moiré occur and reliable colour reproduction is not possible. If the positioning of the different separations could be done with a maximum axial positioning error of about 15μm and a maximum tangential positioning error of about 20μm, better micro-smoothness would be obtained and no moiré would occur. Since positioning of the different separations can not be done this accurate, so called register independent screens, are needed to avoid interference between the different colour separations.

Colours reproduced with register-independent dither screens maintain there colour, independent of the positioning errors between the different colour separations. This is obtained by positioning of the thresholds in the dither matrices in such a way that the halftoned output patterns of the colour separations have different screen angles (see also figure 3.7). By very accurately choosing the different screen angles, disturbing patterns resulting from interference between the different screens are shifted to the high frequency spectrum and therefore become invisible for the human

eye.

As was mentioned in paragraph 3.2.1 a trade-off is necessary between the screen frequency and the number of tone values that can be represented. It was explained that the screen frequency must be high enough in order to make the screen invisible and be able to represent detail. On the other hand it is also desirable to apply a low screen frequency, thereby decreasing the likelihood of false contours. For the dither matrices used in the applied colour technology this trade-off is made, resulting in a minimum difference between successive thresholds, ΔT_m, in dither matrix one of 12, and in the dither matrices two and three of 8 ($0 \leq T \leq 255$). See also appendix A.

It is this difference in the successive thresholds that has to 'buffer' the diffused errors resulting from the error diffusion part of the algorithm in order to completely avoid non-connected (sub)pixels, which are very hard to reproduce and therefore responsible for the noisy impression in halftoned planes. Hence, increment of the threshold multiplication factor λ results in higher relative 'potential barriers' which are more difficult to conquer by the distributed error sum. It follows that the more λ is increased, the more error diffusion influences in the halftoned output image decrease and stable clustered dot ordered dither screens appear. See also figure 5.2. Since the maximum absolute relative error sum $E_{rs}(x,y)$, i.e. the maximum relative error obtained by the pixel under process from already halftoned neighbour pixels, equals 128 ($0 \leq i(m,n) \leq 255$) it can be determined at which multiplication factor λ the influence of the error diffusion algorithm is completely eliminated. So, the magnitude of the multiplication factor λ at which error diffusion influences and therefore non-connected (sub)pixels are completely eliminated (with exception of the very light grey values), called the dither lambda λ_{dith}, can be written as

$$\lambda_{dith} = \frac{| E_{rs}(x,y) |_{max}}{\Delta T_m} \quad , \tag{5.3}$$

where $E_{rs}(x,y)$ represents the relative error sum at location (x,y) and
ΔT_m represents the minimum difference between successive threshold in the dither matrix.

With help of equation 5.3 it follows that $\lambda_{dith} = 10.7$ for dither matrix one and $\lambda_{dith} = 16$ for dither matrices two and three. Hence, when the error diffusion threshold is modulated with its dither matrices multiplied with the different dither lambdas, smooth planes in the original image will be rendered in the halftoned output image by stable and therefore reproducible patterns. It is noted that these high values of lambda guarantee connected (sub)pixels and that the resulting patterns in the halftoned image are exactly the same as those obtained with the clustered dot ordered dither techniques.

Although at these high lambdas stable halftoned output patterns are obtained figure 5.2 also clearly shows that the edge rendering is deteriorated dramatically. This problem is dealt with in the next paragraph.

5.3 Error diffusion with adaptive periodic threshold modulation

From figure 5.2 it clearly follows that for large lambdas the error diffusion influence in the haftoned output image can be eliminated, resulting in stable and good reproducible patterns. Edge rendering however, deteriorates dramatically when these high lambdas are applied.

In order to improve the edge rendering properties it is necessary to detect edges and detail in the original image and halftone this high frequency information with for example the standard error diffusion algorithm, which has good edge rendering properties. So, a segmentation needs to be implemented. The edge and detail information in the original input image is obtained by application of the gradient operator of Prewitt [Vli93] for the *x*- and *y*-direction respectively. See also figure 5.3.

$$\begin{bmatrix} -1 & 0 & 1 \\ -1 & 0 & 1 \\ -1 & 0 & 1 \end{bmatrix} \qquad \begin{bmatrix} -1 & -1 & -1 \\ 0 & 0 & 0 \\ 1 & 1 & 1 \end{bmatrix}$$

A **B**

Figure 5.3: Gradient operator of Prewitt for *x*- (A) and *y*-direction (B).

It is mentioned that also a min/ max - filter is implemented in order to perform the segmentation. According to the outcome of the gradient operator the multiplication factor λ is controlled. For very sharp edges lambda equals zero, resulting in standard error diffusion and for the smooth parts of the image which obtain no edges or detail information, lambda equals λ_{dith}. Between these two extremes a smooth transitions takes place according to

$$\lambda(x,y) = \begin{cases} \lambda_{dith}, & gradient(x,y) < D.P. \\ \lambda_{dith} \cdot e^{-\left(\frac{(gradient(x,y)-D.P.)}{sl}\right)^2}, & D.P. \le gradient(x,y) \le E.P. \\ 0 & gradient(x,y) > E.P. \end{cases} \quad (5.4)$$

where λ_{dith} represents the dither lambda (equation 5.3),
D.P. represents the gradient value below which lambda equals the dither lambda,
E.P. represents the gradient value above which lambda equals zero and
sl is a parameter with which the slope of the segmentation curve can be influenced.

From equation 5.4 it follows that with the parameter *sl* the slope of the curve and therefore the transition smoothness can be controlled. Experimentally it is determined that the applied gradient operation results for smooth planes in values less then 35 (*D.P.* = 35) and for edges or information that needs to be rendered very sharply in values larger then 110 (*E.P.* = 110). In figure 5.4 the normalized segmentation curve of equation 5.4 is depicted for *sl* = 35 and *D.P.* = 35. It is shown that when the gradient increases, meaning stronger edges or more detail information, the multiplication factor λ decreases. This means that high frequency information in the original image, like edges and detail, will be halftoned according to pure error diffusion. It is therefore expected that application of this adaptive periodic threshold modulation technique will

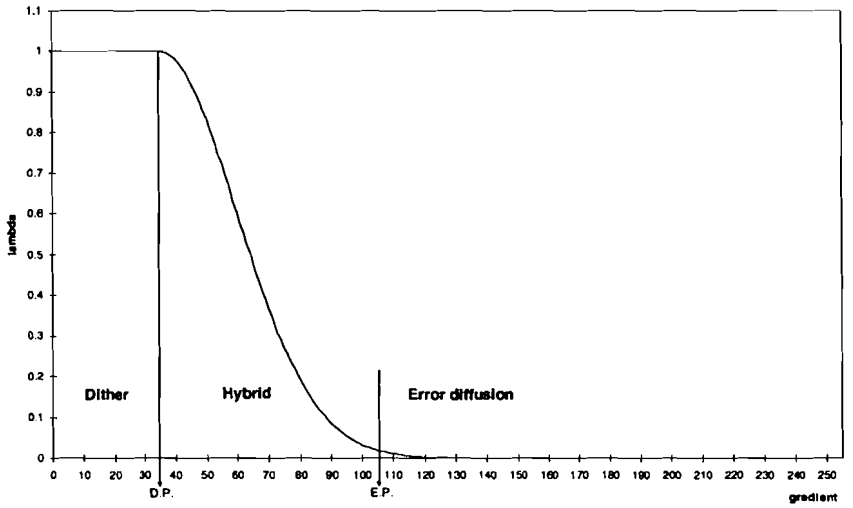

Figure 5.4: Segmentation curve.

result in improved edge rendering. The above segmentation curve is implemented and different experiments were performed.

In figure 5.5 an example of a constant continuous tone plane (40%) halftoned with the adaptive periodic threshold modulation technique is shown. It follows that the edges are rendered well as well as the centre of the plane, which is represented by stable and good reproducible output patterns.

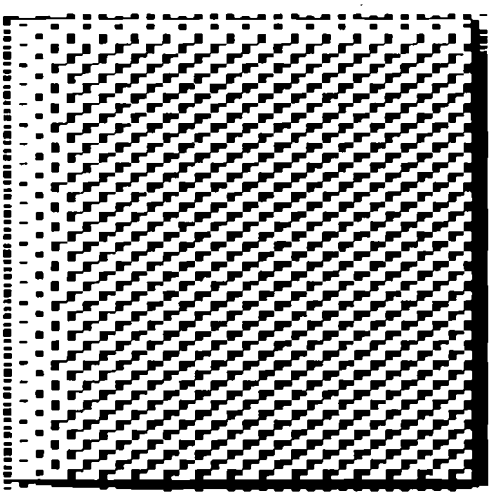

Figure 5.5: Example of constant continuous tone plane halftoned with error diffusion with adaptive periodic threshold modulation ($\lambda_{max}(x,y) = \lambda_{dith} = 16$).

It follows from figure 5.5 however, that a new problem has occurred. Although the edges and the centre of the plane are rendered well some 'in- and out-run phenomena', the white or black

bands at the left, right, top and bottom of the plane, appear. This effect is also shown in figure 5.6 in which the edge enhancement properties of the algorithm are depicted. The same experiments as described in paragraph 3.3.1 were performed.

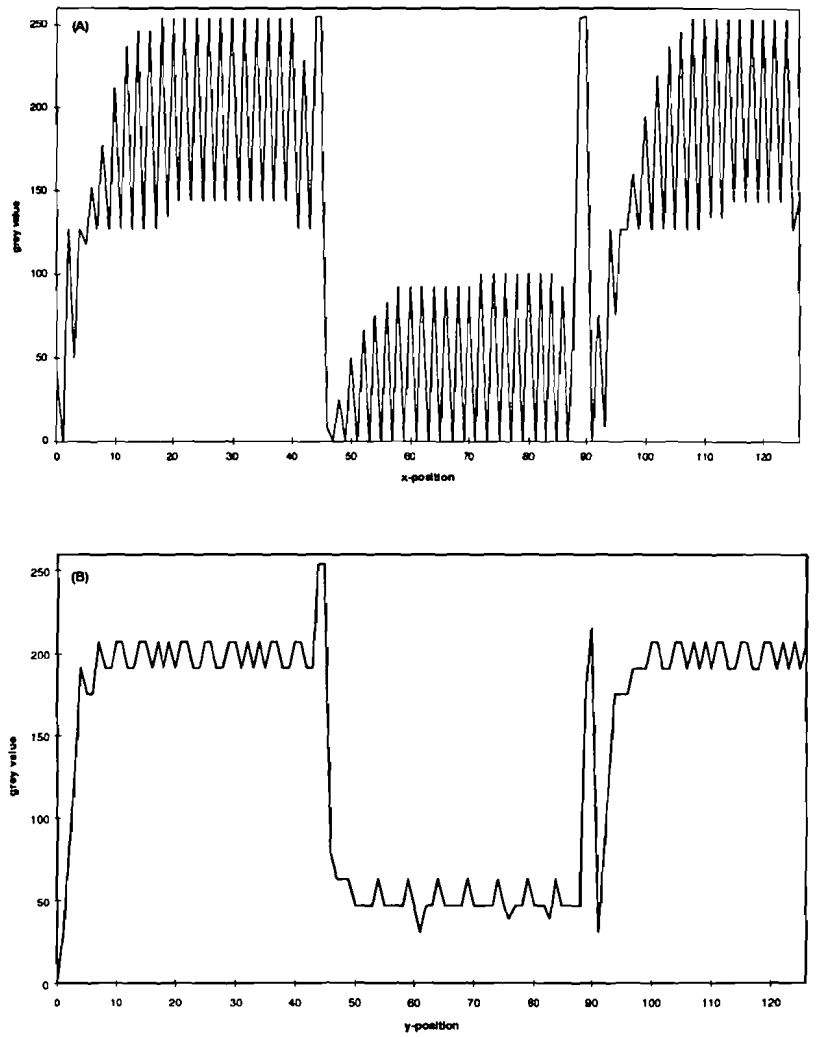

Figure 5.6: Edge rendering properties of error diffusion with adaptive periodic threshold modulation for a horizontal edge (A) and a vertical edge (B) with ($\lambda_{max}(x,y) = \lambda_{dith} = 16$).

The rising average grey levels shown in figure 5.6 clearly show the above ascertained in- and out-run phenomena. Because of the very high lambdas in these smooth regions the with previous made errors corrected input tone value has to built up until it reaches the same dynamic range as the thresholds in the with λ multiplied dither matrix. Till this point is reached the represented grey level will be too low and the resulting average tone value will not (yet) equal the continuous tone value of the input image. It is noted that this correction takes place by means of the error feedback property of the algorithm. See also figure 5.7. When the same dynamic range as the thresholds in the with λ multiplied dither matrix is reached, the resulting output patterns become stable and the average grey levels equal the continuous tone values.
The spikes in figure 5.6 are caused by the regular patterns which result from the combination of

the tone value that needs to be represented and the way the dither matrix is filled in. Figure 5.7 clearly shows the error build-up (white band) and derogation (black band).

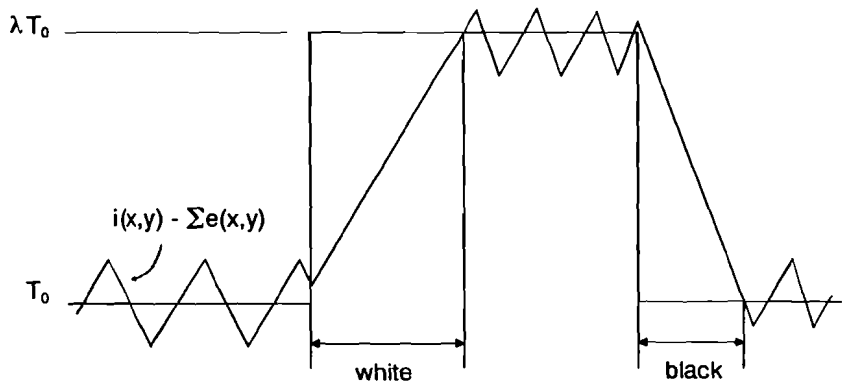

Figure 5.7: In- and out-run phenomena.

Since this artifact can not easily be compensated for only dither lambdas with a maximum value equal to one are allowed in order to avoid the very disturbing in- and out-run phenomena. As was already explained in paragraph 5.1 this does result in clustering of the resulting halftoned output patterns but does not exclude the possibility of non-connected (sub)pixels, which result in output images that obtain a noisy impression and that are hard to reproduce. Because these non-connected (sub)pixel are caused by the error distribution, they can be eliminated by switching this error distribution off. When this is done as function of the gradient it is possible to obtain good edge and detail rendering as well as stable output patterns in smooth planes. Figure 5.8 shows the implemented error extinction curve as function of the gradient. The implemented error extinction curve can be written as

$$d(x,y) = \begin{cases} 0, & gradient(x,y) < D.P. \\ \dfrac{gradient(x,y)}{E.P. - D.P.} - \dfrac{D.P.}{E.P. - D.P.}, & D.P. \le gradient(x,y) \le E.P., \\ 1, & gradient(x,y) > E.P. \end{cases} \quad (5.5)$$

where *d(x,y)* represents the error extinction factor. See also figure 5.8.

Hence, as the gradient increases the error extinction curve also increases, resulting in clustered dot ordered dither for smooth planes (*d(x,y)* = 0, therefore no error distribution and $\lambda(x,y)$ = 1) and error diffusion for edge and detail information (*d(x,y)* = 1 and $\lambda(x,y)$ = 0). When the segmentation curve given in equation 5.4 and the error extinction curve given in equation 5.5 are combined it is possible produce sharp and good reproducible halftoned output images. It is mentioned that it is not necessary to completely switch off the error distribution. A small amount of the error, which can be 'buffered' by the minimum threshold difference, can still be distributed.

In figure 5.9 a constant continuous tone plane (40%), halftoned according to the adaptive periodic threshold modulation algorithm as described above, is depicted. When figure 5.9 is compared with figure 5.5 it becomes clear that the in- and out-run phenomena are eliminated and a good reproducible and sharp halftoned output image results.

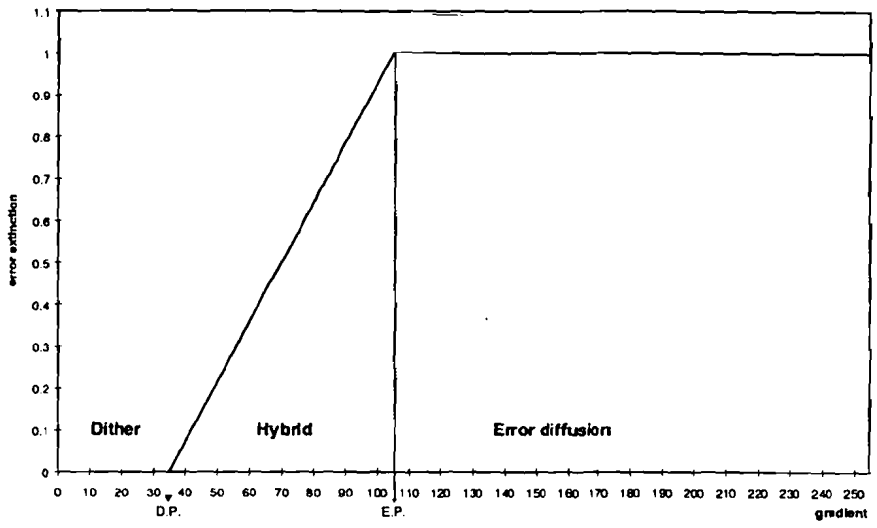

Figure 5.8: Error extinction factor.

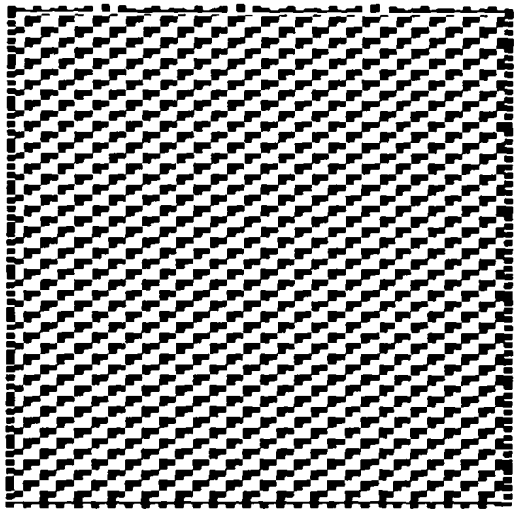

Figure 5.9: Example of constant continuous tone plane halftoned with error diffusion with adaptive periodic threshold modulation ($\lambda_{max}(x,y) = \lambda_{dith} = 1$).

In order to examine the edge enhancement properties of this adaptive periodic threshold modulation technique a horizontal and vertical edge were processed, as described in paragraph 3.3.1. The normalized ratios, representing the average grey values are represented, for the horizontal and vertical edge are depicted in figure 5.10[a] and 5.10[b], respectively.

Figure 5.10 shows that when the amount of error distribution is also controlled by means of the gradient (see figure 5.8) low dither lambdas can be applied, eliminating the in- and out-run

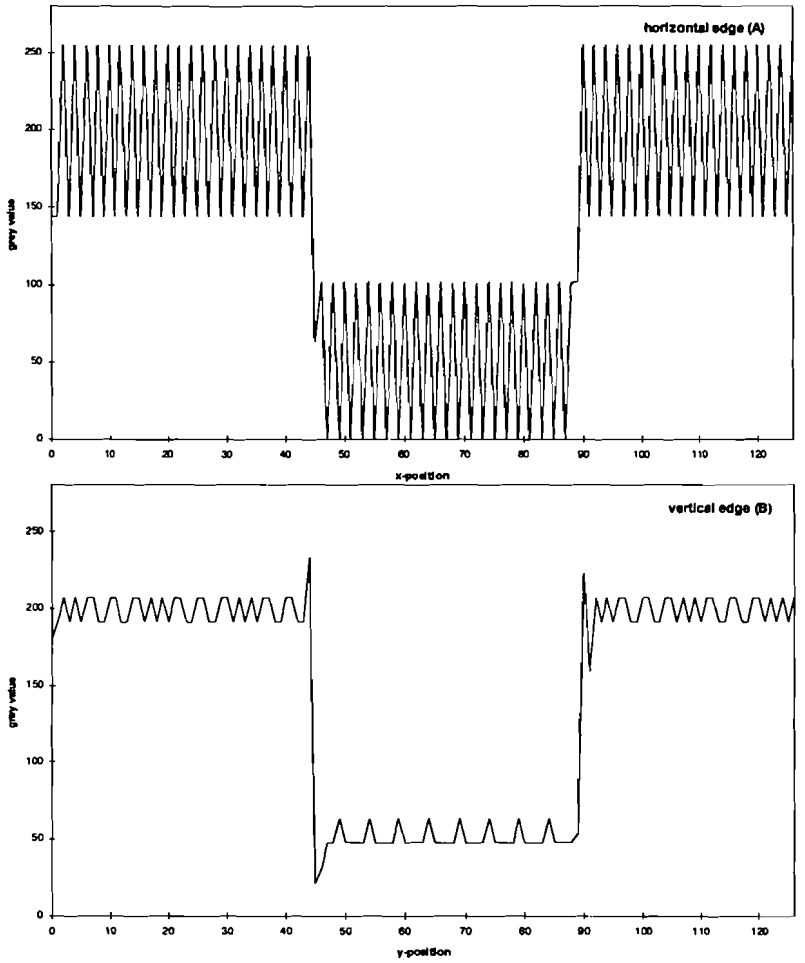

Figure 5.10: Edge rendering properties of error diffusion with adaptive periodic threshold modulation for a horizontal edge (A) and a vertical edge (B) with ($\lambda_{max}(x,y)$ = λ_{dith} = 1).

phenomena shown in figure 5.5 and 5.6, while clustering of the output pixels as well as good edge rendering is guaranteed. The over- and undershoot shown in figure 5.10[b] indicate the good edge and detail rendering properties. In figure 5.10[a] however, the edge enhancement properties can be improved by extension of the 'edge region' or by application of an error diffusion threshold T_0 which equals 128 instead of 0. In order to obtain the correct average grey levels the new threshold is given by

$$T(m,n) = T_0 + \lambda . (cell(m,n) - T_0) , \qquad (0 \le \lambda \le 1) \qquad (5.6)$$

where T_0 represents the fixed (error diffusion) threshold.

The resulting edge rendering properties are depicted in figure 5.11. It is shown that the edge and detail rendering properties improve by application of a fixed error diffusion threshold T_0 that

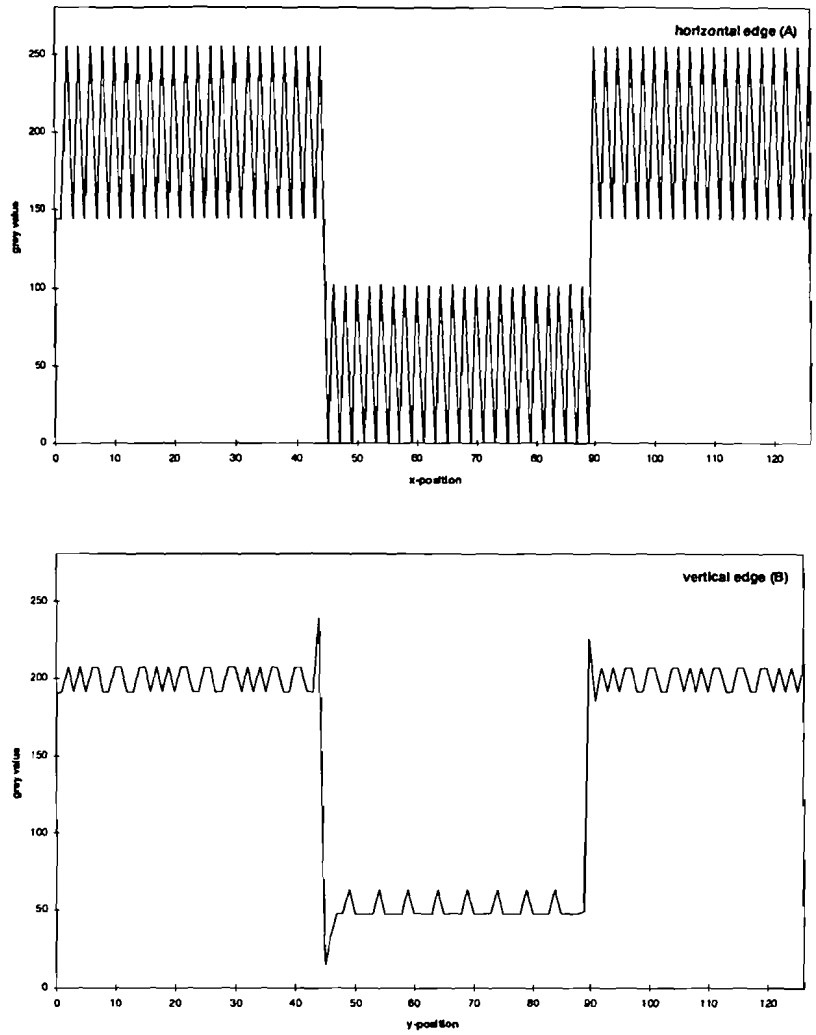

Figure 5.11: Edge rendering properties of error diffusion with adaptive periodic threshold modulation for a horizontal edge (A) and a vertical edge (B) with ($\lambda_{max}(x,y) = \lambda_{dith} = 1$ and $T_0 = 128$).

equals 128. Especially the horizontal edges will be rendered better because 'in-run' phenomena resulting from an error diffusion threshold equal to zero are eliminated immediately, which is important for processing over a few edge pixels.

It is mentioned that when the original image is processed along a serpentine raster the edge rendering properties are, although more symmetric (see also paragraph 3.3.2), equal to processing along the traditional raster. Directional artifacts resulting from the error diffusion algorithm do not appear because smooth planes will be halftoned according to clustered dot ordered dither and therefore processing according to the serpentine raster is not necessary.

Hence, sharp as well as stable and therefore good reproducible halftoned output images can be obtained by application of this adaptive periodic threshold modulation technique. It is noted that

because the error distribution property is (almost) switched off when smooth planes need to be rendered, the average tone value will deviate from the tone values in the original image. By application of dither matrices that are large enough to prevent contouring artifacts however, this resulting error is acceptable.

In figure 5.12 an image processed with clustered dot ordered dither, adaptive periodic threshold modulation and pure error diffusion is depicted. It is shown that the adaptive periodic threshold modulation variant obtains the edge rendering properties of pure error diffusion and the stability of clustered dot ordered dither.

It is mentioned that by monitoring the error sum, i.e. the total error obtained by the pixel under process from its neighbour pixels, it should be possible to correct for the in- and out-run phenomena which occur when large lambdas are applied. Although this should make application of large lambdas, without the introduction of disturbing artifacts, possible, it is expected that this will result in equal image quality as when the above adaptive periodic threshold modulation technique is applied. This becomes clear when it is considered that by applying large lambdas the error distribution in fact also is eliminated.

5.4 Conclusions

In order to obtain halftoned output images which have the edge enhancement properties of error diffusion and are also good reproducible, an adaptive periodic threshold modulation technique is developed. Based on a gradient the amount of threshold modulation as well as the amount of error distribution is controlled, resulting in the desired output patterns. For smooth planes the dither matrices are imposed and the error distribution is switched off, resulting in a stable and therefore visible pleasing, representation of this slowly varying or smooth information. High frequency information, like edges and detail, are halftoned according to pure error diffusion, resulting in good edge rendering in the halftoned output image. From the performed experiments it is concluded that application of this adaptive periodic threshold modulation technique results in stable, good reproducible and visually pleasing output patterns which lack the noisy impression resulting from pure error diffusion, but obtain the edge rendering properties of pure error diffusion. Because different dither matrices are used for different colours, stable and reliable colour mixing is obtained.

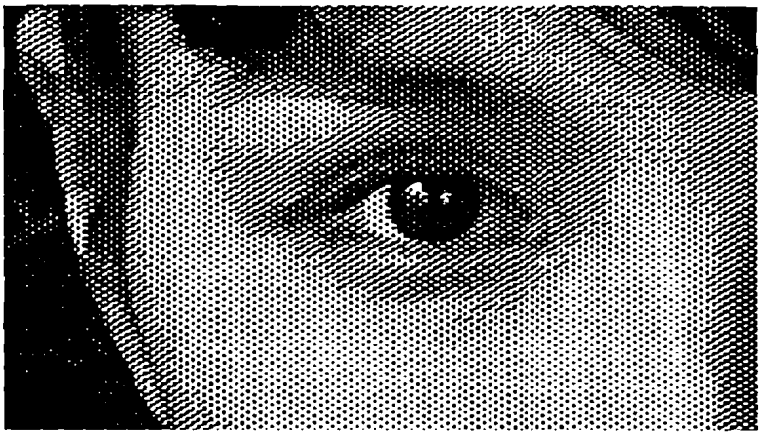

A

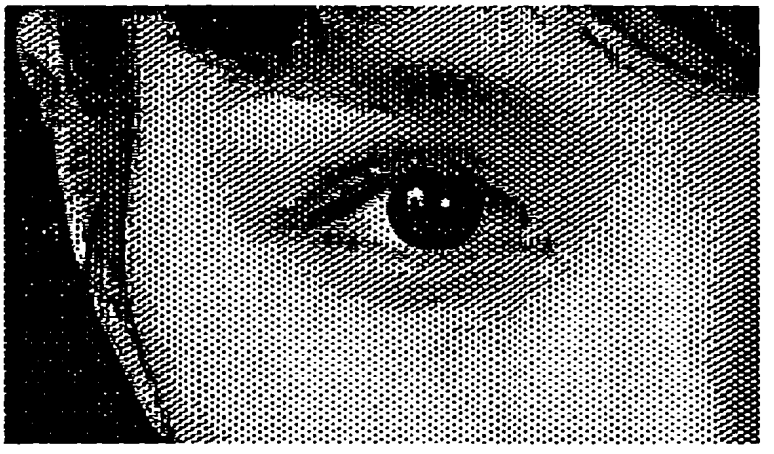

B

C

Figure 5.12: Image processed with clustered dot ordered dither (A), adaptive periodic threshold modulation (B) and pure error diffusion (C).

Chapter 6

Conclusions

In order to reproduce high quality output images, different techniques which convert the continuous tone information, representing the original image, to bi-level output images, necessary for reproduction on most copiers and printers, exist. An overview of the most commonly used so called halftone techniques is given in table 6.1.

Table 6.1: Classification of halftone techniques

	Screening		Ordered dither/ masking		Error diffusion	
	Clustered dot	Dispersed dot	Clustered dot	Dispersed dot	Clustered dot	Dispersed dot
Regular structures	Traditional screening		Clustered dot ordered dither			
Irregular structures				Baker dither Void and cluster method Blue Noise masking	Error diffusion plus hysteresis Error diffusion with periodic threshold modulation	Error diffusion (perturbations in threshold, error filter and raster direction)

When high quality output images need to be reproduced dispersed dot halftone techniques, which result in irregular structures, are preferred. These techniques produce halftone textures with energy predominantly in the very high spatial frequencies, which therefore result in images that are very pleasing to the human eye. When these techniques are implemented however, limitations of the print engine used to reproduce these images can become a major problem. If the very fine, high frequency patterns in the halftoned output image can not reliably be printed, the resulting output obtains a noisy impression, which is visually very disturbing. Hence, in order to obtain maximum image quality it is necessary to apply halftone techniques that produce output patterns which obtain printable irregular structures. From table 6.1 it follows that error

diffusion plus hysteresis and error diffusion with periodic threshold modulation should obey these demands. In order to examine the applicability of these halftone techniques, both algorithms as well as modifications to these algorithms are implemented in software and different experiments were performed.

It is concluded that modulation of the error diffusion threshold by an output dependent feedback term does not result in the required high quality halftoned output images. Although good edge rendering is obtained, visually disturbing artifacts occur because of the instability of the algorithm. It was shown that it is impossible to guarantee a minimum average runlength, necessary for high quality image reproducibility, without introducing other visually disturbing artifacts. Another major drawback of this output dependent feedback technique is that because of the vertical structures that arise from the hysteresis term the different colour separations become register dependent, which makes reliable and artifact free colour mixing next to impossible. It is therefore concluded that application of pure error diffusion or error diffusion with output dependent feedback will not, on the applied print engine, result in visually pleasing high quality output patterns. First when the resolution and reproducibility of individual subpixels is improved pure error diffusion might result in the desired image quality.

In order to eliminate the noisy impression that occurs when error diffusion (with hysteresis) is applied while maintaining the edge enhancement properties, an adaptive periodic threshold modulation technique is implemented. It is shown that by making use of an edge operator in order to control the amount of threshold modulation and the error extinction factor, sharp and reproducible output images can be obtained. Because different dither matrices are used for the different colour separations reliable colour mixing is possible. It is mentioned that better edge rendering properties can be obtained by thickening of the edges, which will result in a larger amount of pure error diffusion in the halftoned output image.

References

[Bay73] Bayer, B.E.
An optimum method for two-level rendition of continuous tone pictures
IEEE International Conference on Communications, Vol. 1, pp. 26/11-26/15, 1973

[Dou94] Dougherty, E.R.
Digital image processing methods
New York: Marcel Dekker, 1994

[Esc94] Eschbach, R.
Pixel-based error diffusion algorithm for producing clustered halftone dots
Journal of Electronic Imaging, Vol. 3(2), pp.198-202, April 1994

[Flo76] Floyd, R.W. and L. Steinberg
An adaptive algorithm for spatial grayscale
Proceedings SID, Vol. 17(2), pp.75-77, 1976

[Jon94] Jones, P.R.
Evolution of halftoning technology in the United States patent literature
Journal of Electronic Imaging, Vol. 3, No. 3, pp. 257-275, July 1994

[Kno93[1]] Knox, K.T.
Error diffusion: a theoretical view
Proceedings SPIE Human Vision, Visual Processing and Digital Display IV,
Vol. 1913, pp.326-331, February 1993

[Kno93[2]] Knox, K.T.
Threshold modulation in error diffusion
Journal of Electronic Imaging, Vol. 2(3), p.185-192, July 1993

[Lev91] Levien, R.L.
Photographic image reproduction device using digital halftoning to scrren images allowing adjustable coarseness
US Patent 5.055.942
October 8, 1991

[Mit92] Mitsa, T. and K.J. Parker
Digital halftonig technique using a blue-noise mask
Journal Optical Society of America A, Vol. 9, No. 11, pp.1920-1929, November 1992

[Par92] Parker, K.J. and T. Mitsa
Method and apparatus for halftone rendering of a gray scale image using a blue noise mask
Assignee: Research Technologies Corporation, Inc., Tucson, Arizona
US Patent, No. 5,111,310
May 5, 1992

[Stof81] Stoffel, J.C. and J.F. Moreland
A survey of electronic techniques for pictorial image reproduction
IEEE Transactions on Communications, Vol. Com-29, No.12, pp.1898-1925, December 1981

[Sch84] Scheuter K.R. and G. Fischer
Frequency modulation picture rendering with random pixel distribution
In: Photographic and electronic image quality, Proc. Symp., pp. 154-160, Cambridge University, 10 - 14 September 1984
Published by the Science Committee of the Royal Photographic Society, November 1984

[Uli87] Ulichney, R.
Digital Halftoning
Cambridge, Massachusetts: The MIT Press., 1987

[Uli88] Ulichney, R.
Dithering with blue noise
Proceedings of the IEEE, Vol. 76, No. 1, pp.56-79, January 1998

[Uli93] Ulichney, R.
The void-and-cluster method for dither array generation
Proceedings SPIE Human Vision, Visual Processing and Digital Display IV, Vol. 1913, pp. 332-343, February 1993

[Vli93] Vliet van, R.G.
Beeldbewerking
Eindhoven (The Netherlands): Eindhoven University of Technology, 1993
Lecture Notes

[Wid92] Widmer, E. et al
The benifits of frequency modulation screening
Technical Association of the Graphic Arts, Proceedings I, pp.28-43, 1992

[Yao94] Yao, M. and K.J. Parker
Modified approach to the construction of a blue noise mask
Journal of electronic imaging, Vol. 3, No. 1, pp. 92-97, January 1994

Acknowledgements

From August 1, 1995 until March 15, 1996 I have performed my graduation work at Océ van der Grinten N.V., department Research and Development, in Venlo, as final part of the study Electrical Engineering at the Eindhoven University of Technology in The Netherlands. This report describes most of the work I performed during the past seven and a half months.

My thanks go out to Océ, for giving me the opportunity to perform my graduation work and the many people who have contributed to the result by helping and motivating me. In particular I would like to thank Rom van Strijp, my mentor, for making this work possible and Ronald Fabel for the many sensible, sometimes absurd, but always interesting discussions. Finally, I thank ir. N.G.M. Kouwenberg at the Eindhoven University of Technology for accepting the difficult task of external mentor and prof. dr. ir. P.P.J. van den Bosch for supervising my graduation work.

Appendix A

Dither matrices for the different colours

A.1 Dither matrix one

0	15	31	46	0	15	31	46
3	18	34	49	3	18	34	49
6	21	37	52	6	21	37	52
9	24	40	55	9	24	40	55
12	27	43	58	12	27	43	58
30	45	2	17	30	45	2	17
33	48	5	20	33	48	5	20
36	51	8	23	36	51	8	23
39	54	11	26	39	54	11	26
42	57	14	29	42	57	14	29
1	16	32	47	1	16	32	47
4	19	35	50	4	19	35	50
7	22	38	53	7	22	38	53
10	25	41	56	10	25	41	56
13	28	44	59	13	28	44	59
31	46	0	15	31	46	0	15
34	49	3	18	34	49	3	18
37	52	6	21	37	52	6	21
40	55	9	24	40	55	9	24
43	58	12	27	43	58	12	27
2	17	15	45	2	17	15	45
5	20	18	48	5	20	18	48

A.2 Dither matrix two

18	47	73	13	39	68	8	34	60	**0**
21	50	76	16	42	71	11	37	63	3
24	53	79	19	45	74	14	40	66	6
27	56	82	22	48	77	17	43	69	9
30	59	85	25	51	80	20	46	72	12
33	62	**2**	28	54	83	23	49	75	15
36	65	5	31	57	86	26	52	78	18
39	68	8	34	60	**0**	29	55	81	21
42	71	11	37	63	3	32	58	84	24
45	74	14	40	66	6	35	61	**1**	27
48	77	17	43	69	9	38	64	4	30
51	80	20	46	72	12	41	67	7	33
54	83	23	49	75	15	44	70	10	36
57	86	26	52	78	18	47	73	13	39
60	**0**	29	55	81	21	50	76	16	42
63	3	32	58	84	24	53	79	19	45
66	6	35	61	**1**	27	56	82	22	48
69	9	38	64	4	30	59	85	25	51
72	12	41	67	7	33	62	**2**	28	54
75	15	44	70	10	36	65	5	31	57
78	18	47	73	13	39	68	8	34	60
81	21	50	76	16	42	71	11	37	63
84	24	53	79	19	45	74	14	40	66
1	27	56	82	22	48	77	17	43	69
4	30	59	85	25	51	80	20	46	72
7	33	62	**2**	28	54	83	23	49	75
10	36	65	5	31	57	86	26	52	78
13	39	68	8	34	60	**0**	29	55	81
16	42	71	11	37	63	3	32	58	84

A.3 Dither matrix three

0	60	34	8	68	39	13	73	47	18
3	63	37	11	71	42	16	76	50	21
6	66	40	14	74	45	19	79	53	24
9	69	43	17	77	48	22	82	56	27
12	72	46	20	80	51	25	85	59	30
15	75	49	23	83	54	28	**2**	62	33
18	78	52	26	86	57	31	5	65	36
21	81	55	29	**0**	60	34	8	68	39
24	84	58	32	3	63	37	11	71	42
27	**1**	61	35	6	66	40	14	74	45
30	4	64	38	9	69	43	17	77	48
33	7	67	41	12	72	46	20	80	51
36	10	70	44	15	75	49	23	83	54
39	13	73	47	18	78	52	26	86	57
42	16	76	50	21	81	55	29	**0**	60
45	19	79	53	24	84	58	32	3	63
48	22	82	56	27	**1**	61	35	6	66
51	25	85	59	30	4	64	38	9	69
54	28	**2**	62	33	7	67	41	12	72
57	31	5	65	36	10	70	44	15	75
60	34	8	68	39	13	73	47	18	78
63	37	11	71	42	16	76	50	21	81
66	40	14	74	45	19	79	53	24	84
69	43	17	77	48	22	82	56	27	**1**
72	46	20	80	51	25	85	59	30	4
75	49	23	83	54	28	**2**	62	33	7
78	52	26	86	57	31	5	65	36	10
81	55	29	**0**	60	34	8	68	39	13
84	58	32	3	63	37	11	71	42	16